REPORT DOCUMENTATION PAGE

AFRL-SR-BL-TR-00-

0350

1. REPORT DATE (DD-MM-YYYY)	2. REPORT TYPE	3. DATES COVERED (From - To)
28-07-2000	Final Technical Report	01 May 1997 - 30 April 2000

4. TITLE AND SUBTITLE
(New World Vistas) Research on Intense, Photoconductively-Switched Stacked Blumlein Modulators to Supply Ultra-Wideband HPM Systems

5a. CONTRACT NUMBER

5b. GRANT NUMBER
F49620-97-1-0260

5c. PROGRAM ELEMENT NUMBER

6. AUTHOR(S)
Carl B. Collins
Farzin Davanloo

5d. PROJECT NUMBER

5e. TASK NUMBER

5f. WORK UNIT NUMBER

7. PERFORMING ORGANIZATION NAME(S) AND ADDRESS(ES)
The University of Texas at Dallas
2601 North Floyd Road
P.O. Box 830688
Richardson, Texas 75083-0688

8. PERFORMING ORGANIZATION REPORT NUMBER

9. SPONSORING / MONITORING AGENCY NAME(S) AND ADDRESS(ES)
Air Force Office of Scientific Research
AFOSR/NE
801 North Randolph Street, Room 732
Arlington, VA 22203-1977

10. SPONSOR/MONITOR'S ACRONYM(S)

11. SPONSOR/MONITOR'S REPORT NUMBER(S)

12. DISTRIBUTION / AVAILABILITY STATEMENT
Approved for public release; distribution unlimited

20000804 204

13. SUPPLEMENTARY NOTES

14. ABSTRACT
In this work, Several photoconductively- switched stacked Blumlein prototype were developed and successfully tested at power levels approaching 100 MW. These devices had a compact geometry and commutated by a single avalanche photoconductive switch. Special attention was placed on broadening of the switch current channels. Device longevity was tested by fabricating switch with metal or diamond coatings and by implementing different switch/electrode configurations. A significant improvement in switch lifetime was resulted by testing the diamond-coated switch performance in a prototype pulser. In order to obtain an understanding of electrical conduction mechanisms, semiconductor properties of amorphic diamond coatings were examined. Deposition of thin films of amorphic diamond on both Si and GaAs crystalline substrates produced rectifying heterojunctions with highly asymmetric current-voltage characteristics.

15. SUBJECT TERMS
Stacked Blumlein Pulsers, Amorphic Diamond, High Gain GaAs Phoconductive Semiconductor Switch, Photoconductive Switching, High Power Repetitive Pulsers, Rectifying Heterojunction

16. SECURITY CLASSIFICATION OF: Unclassified			17. LIMITATION OF ABSTRACT	18. NUMBER OF PAGES	19a. NAME OF RESPONSIBLE PERSON
a. REPORT	b. ABSTRACT	c. THIS PAGE			Farzin Davanloo
U	U	U	SAR	79	19b. TELEPHONE NUMBER (include area code) (972)883-2863

14. Abstract continued

When reversed biased, current levels from the heterojunction varied with the amount of reverse bias and the illumination and a photoconductive effect was observed. Measurements indicated an electrical breakdown strength of better than 3 x 10^9 V/m for the amorphic diamond. The diamond/Si heterojunction devices were tested as photoconductive switches in our Blumlein pulsers where they successfully commutated the pulsers at low powers.

Final Technical Report

describing

Research for U.S. Air Force Office of Scientific Research (AFOSR)

entitled

"(New World Vistas) Research on Intense, Photoconductively - Switched Stacked Blumlein Modulators to Supply Ultra - Wideband HPM Systems"

for the period

5/1/97 through 4/30/00

Grant No: F49620-97-1-0260

Principal Investigators:

C. B. Collins
F. Davanloo

Center for Quantum Electronics
University of Texas at Dallas
P.O. Box 830688, Richardson, TX 75083-0688

TABLE OF CONTENTS

INTRODUCTION 2

PHOTOCONDUCTIVE SWITCHING OF STACKED BLUMLEIN PULSERS 9

- Stacked Blumlein Prototypes Commutated by a Photoconductive Switch 9
- Laser Diode Activation 18
- Improvements to Charging Pulse Compression Module (CPC) 19
- Pulser Operation 23
- True Field Probing of the Waveforms 27

SWITCH LIFETIME CONSIDERATION AND STUDIES 33

- Avalanche Initiations and Current Filamentation 33
- Switch Contact Deposition 35
- Amorphic Diamond Coating of GaAs Switches – Concept 35
- Switch Lifetime Studies with Metal Contacts 42
- Switch Lifetime Studies Using Amorphic Diamond 51

AMORPHIC DIAMOND COATINGS 55

- General Properties 55
- Semiconductor Properties of Amorphic Diamond
  - Field emission 57
  - Formation of rectifying heterojunctions 61

CONCLUSIONS 72

EXECUTIVE SUMMARY 75

- Summary of the Results 75
- Personnel Participated 76
- Publications 76

REFERENCES 78

INTRODUCTION

Most pulsed power sources function by storing at a slow rate from a regular supply, then delivering it in relatively shorter pulses to a load. This repetitive process allows the attainment of high power levels for short periods of time, creating operating conditions for various modern applications. Specific output characteristics depend on the design and construction of the individual elements comprising each device. A typical pulsed power generator consists of an energy unit, such as a capacitor, inductor, or chemical bank, followed by a shaping section, usually a pulse forming line (PFL), which tailors each pulse to the desired specification and delivers it to the load. The discharge and delivery mechanism is usually triggered on demand using a high voltage switch, such as a thyratron or a spark gap.

Commonly used PFLs are generally made up of simple transmission lines or, in some cases, Blumleins, which are composed of two transmission lines with a common high voltage conductor [1]. An important and attractive Blumlein property is the fact that it can combine the function of pulse shaping with that of energy storage, thus reducing the complexity of the system.

Extensive experiments have been performed at the University of Texas at Dallas (UTD) to develop high power pulses having Blumleins as constituents of the storage and pulse shaping sections. In 1986, the UTD group succeeded in switching a 1 Ω Blumlein with a hydrogen thyratron at a repetition rate of 100 Hz [2-4]. This pulser was used to power an x-ray diode with a low geometric profile, which had the capability of operating over a large portion of the x-ray spectrum. The photon energy range accessible using this pulser and diode combination spanned from 5 to 100 keV. However, for applications requiring higher energies, operating parameters for the single Blumlein pulse power device were constrained by the limitation on voltage hold-

off of commercially available thyratrons. One way for this Blumlein device to access x-ray energies above 100 keV was to commutate the pulser at voltages above 100 kV, which is outside the functional range of the thyratron used. Another method was to include some type of voltage multiplication circuitry in the pulser itself in order to increase the total output voltage.

In an attempt to access higher voltages, we introduced in 1988 an early version of stacked Blumlein pulser [5,6]. The device consisted of several flat-plate Blumleins that were charged in parallel using a regular power supply. All lines were than synchronously discharged using a single hydrogen thyratron, allowing their outputs to add across the series connection for an increase in peak voltage. This device was capable of delivering high-voltage pulses at high repetition rates without putting much stress on any one element.

Early prototypes of the stacked Blumlein pulse generators were used to produce short bursts of intense x-rays. They were carefully modified and improved in order to optimize x-ray outputs. In order to study the pulser and its feasibility for various other applications, a study was initiated concentrating on the stacked Blumlein and parameters that control the output current and its dependence on time. The characterization of the pulser focused on the dependence of output pulse features on several device parameters. These included the type of switching element and the number of Blumlein lines, as well as the line length and configuration [7]. Several different thyratrons and a fast spark gap were used to examine the effects of various switch characteristics on the output. The number and the length of the Blumleins were varied, and the devices were operated and analyzed before and after stacking. It was found that the width of the output pulse could be controlled by varying the length of the Blumleins. High voltage pulses as long as 600 ns were produced without degradation of device voltage gain [8].

In order to estimate the lifetime of the components of the pulser, a test Blumlein device was operated at high voltage and repetition rates, purposely inflicting a high stress on the dielectric boards and other potentially vulnerable components [8]. In a different direction, studies were performed to demonstrate the possibility of reducing the volume, weight, and cost of stacked Blumlein generators [8].

These previous studies showed that, because of their unique characteristics, the UTD stacked Blumlein pulse generators seemed to be excellent power sources for a variety of functions. While their versatility in the production of x-ray had already been demonstrated, many possible uses, such as driving high-power microwave (HPM) loads, had yet to be investigated. Some modern application, such as the generation of ultra-wide band HPM, require the generation of nanosecond wide electric pulses with higher repetition rates and risetimes less than one nanosecond, which were unattainable with conventional thyratrons or spark gaps. However, it seemed that previous performance could be pushed further, to satisfy these conditions. Pulsed sources that can combine these new parameters with the high-voltage performance and practicality of stacked Blumlein in compact packages are of considerable interest.

The segment of the pulser that dictates the limits on much of its performance is the switch used for commutation. For example, the high-pressure gas switch [9] could fit the requirement discussed above if used with low-impedance loads. However, due to their geometry and the necessary precautions associated with high pressure gases, devices using this particular switch are large and impractical. The best promise seems to lie in the concept of a high voltage, photoconductive semiconductor switch (PCSS) capable of being triggered on demand [10]. However, when high-voltage pulses with very fast risetimes are required, conventional linear

photoconductive switch technology are limited by the time necessary to produce enough charge carriers for commutation. Under normal circumstances, a photoconductive switch is nonconductive, thereby allowing the establishment of a high electric field across the semiconductor material between switch electrodes. A laser can then be used to provide trigger photons that are absorbed and create free charge carriers, changing the switch into a conductor.

It has been observed in GaAs PCSS that, as the field across the electrode gap is increased, there is a threshold above which absorbed photons will initiate a fast, non-linear, avalanche process within the material. In this case, a great many carriers are produced for each absorbed photon, and the switch continues to conduct for as long as the field remains across the device. The main differences between linear and avalanche processes are the laser energies used to trigger the switch and the risetime of the generated pulse [11]. In linear switches, the risetime is determined by the speed of the laser. In avalanche type switches, much lower laser energy is used to trigger the switch, after which a very fast carrier multiplication process takes place. The risetime is therefore not dependent on the laser risetime but on the characteristic avalanching time of the device.

Initially, the most common difficulty involved with high gain commutation of stacked Blumlein pulsers was spontaneous, unwanted triggering during the charging cycle. When arranged to operate in avalanche conditions, the switch was subjected to a high electric field for a relatively long time, causing it to leak current, generating heat and ultimately inducing a breakdown and switch failure. As a solution, we have used an intermediary pulser that could charge the photoconductively-switched Blumleins in less than 100 ns, reducing the time of high-voltage pressure on the switch and drastically increasing its lifetime. This charging pulse compression (CPC) module consisted of a tapered Blumlein commutated by a thyratron [12].

During the course of this research program, several photoconductively-switched prototype stacked Blumlein devices capable of generating nanosecond pulses with subnanosecond risetimes were constructed and characterized. Their operating parameters were studied and optimized to find the region in which a GaAs switch could avalanche, producing output voltages approaching 180 kV. Several different commutation assemblies were also used to connect the Blumleins and the switch in a very low impedance geometry which preserved the risetime of the pulse. Modifications to the pulse forming assemblies allowed generation of output waveforms with pulse durations in the range 1-3 ns.

During the avalanche-mode switching of a pulser, the current is concentrated in filaments that extend from the cathode to the anode across the insulating region of the GaAs switch in a lateral configuration [13]. Carrier recombination results in the emission of characteristic band gap photons in the near infrared region that can be seen by an infrared viewer. Filamentary currents with densities of several MA/cm^2 passing through a narrow channel can cause switch damage, especially at the contacts points. A greater number of filaments during each cycle of commutation reduce the stress on the switch, thereby increasing its lifetime.

During this research program, a substantial effort was directed to study and implement the broadening of the current channels in the avalanche photoconductive switch in order to improve lifetime and increase switching peak power. This was performed by two approaches. The first was control of laser diode beam delivery to the switch, and improvements of switch contacts, pulser configuration and charging mechanism. The second approach was the study and use of amorphic diamond film as the switch electrode coating to enhance operation and lifetime of a PCSS in stacked Blumlein pulse generators.

Basic research in our laboratory has described a conformal coating that has hardness of natural diamond and exceptionally high values of electron emissivity [14-21]. Discovered at UTD, it is made from graphite and laser light without catalyst, noxious byproduct, or toxic wastes. It was termed amorphous ceramic diamond and later shortened to "amorphic diamond" for convenience. Deposited at room temperatures it forms a strong bond to any material onto which it is applied. Such a favorable combination of hardness, chemical bonding and an elastic modulus of 850 GPa should translate directly into an increased resistance to abrasive wear of components coated with amorphic diamond. It has been demonstrated that only a 1-3 μm coating of amorphic diamond could protect fragile substrates against erosive environments.

In this work, we studied the use of amorphic diamond film as the PCSS electrode coating to enhance operation and lifetime of the switch. The triggered face of a GaAs switch was over-coated with highly adhesive film of amorphic diamond in order to harden the switch cathode region and improve the avalanche process. A significant improvement in switch lifetime was demonstrated by testing the diamond-coated switch performance in a prototype pulser. We also examined the relevant semiconductor properties of amorphic diamond coatings on conventional crystalline semiconductors. These studies were performed in order to obtain an understanding of the electrical conduction mechanisms that is essential for the utilization of amorphic diamond coatings in the PCSS based pulse power applications.

PHOTOCONDUCTIVE SWITCHING OF STACKED BLUMLEIN PULSERS

Stacked Blumlein pulsers have produced high-power waveforms with risetimes and repetition rates in the range of 0.2-50 ns and 1-200 Hz respectively, using a conventional thyratron, spark gap or photoconductive switch. These devices consist of several triplate Blumleins charged in parallel at one end and discharged in series at the other end by means of a single switch. In this way, relatively low charging voltages are multiplied to give a high discharge voltage across an arbitrary load.

1. Stacked Blumlein Prototypes Commutated by a Photoconductive Switch

Our efforts for this research program have resulted in implementation and demonstration of several intense photoconductively switched stacked Blumlein pulser. These devices operate at switch peak powers of 50-80 MW with laser diode trigger energies as low as 300 nJ. Blumlein prototype pulsers driven by photoconductive switches include: Single Blumlein, 2-line A (version 1), 2-line A, 2-line B, 2-line B with an extended transmission line load, 2-line B (version 2), 2-line C, and 4-line (version 1). Photographs of these pulsers are produced in Figs. 1 - 8. Brief descriptions of these devices used in our current investigations are also given here for reference. These pulsers have been operated with different line impedances, commutation subassemblies, and charging schemes. They were designed and constructed in order to experimentally determine design shortcomings and identify deficiencies so that an optimized device can be produced.

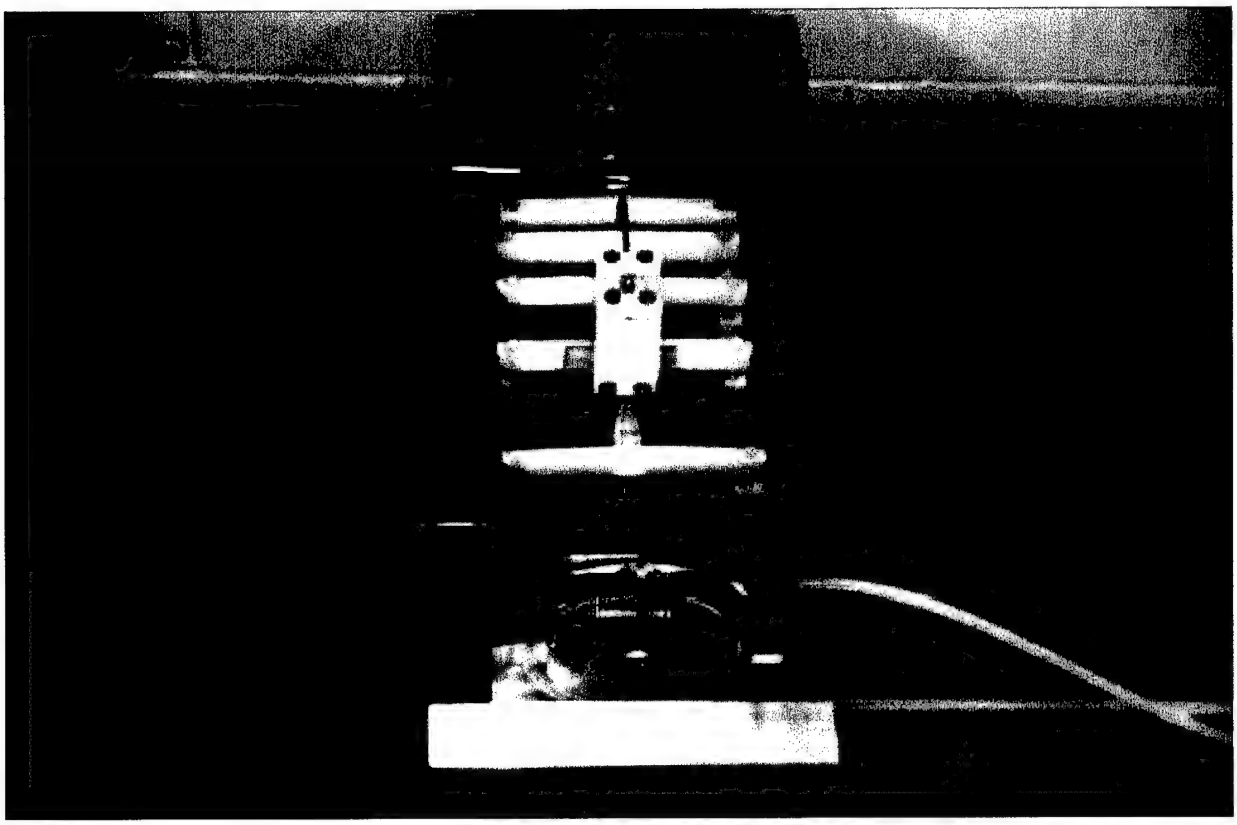

Figure 1. Photograph showing the single Blumlein pulser commutated by a photoconductive switch to produce 60 kV, 5 ns output pulses with risetimes in the range of 200-400 ps. The Blumlein length is 38 cm and line impedance of either 50 Ω or 100 Ω can be utilized.

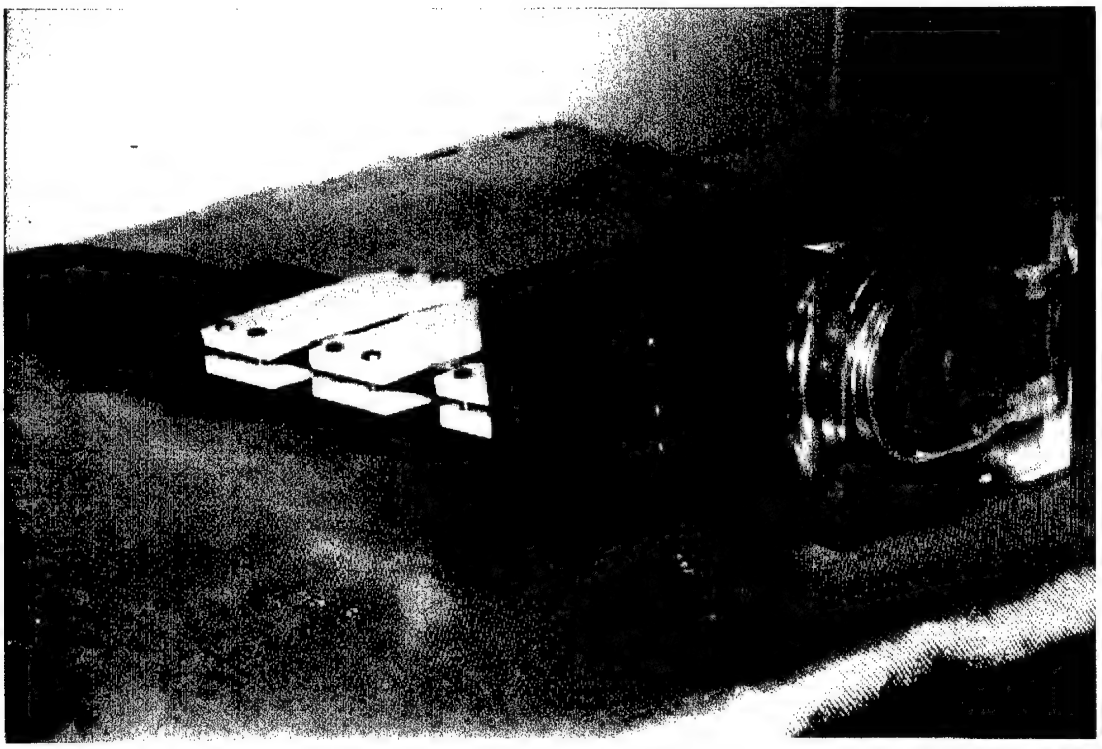

Figure 2. Photograph showing the 2-line A pulser (version 1) commutated by a photoconductive switch. In this device, the corresponding high voltage and ground copper plates for each of the Blumleins are connected together at the switch assembly. Two Blumleins with line impedances of 50 Ω are extended to the close proximity of the stacking location, 45 cm from the switch assembly where they are angled toward each other along with the dielectric for another 5 cm where they are stacked directly on top of one another. The lines are connected in series about 7.5 cm where the top and bottom plates are connected to a resistive load built from a stack of ten, 10 Ω non-inductive carbon disc resistors. The pulser is capable of producing 100 kV, 5 ns output pulses with risetimes in the range of 300-500 ps.

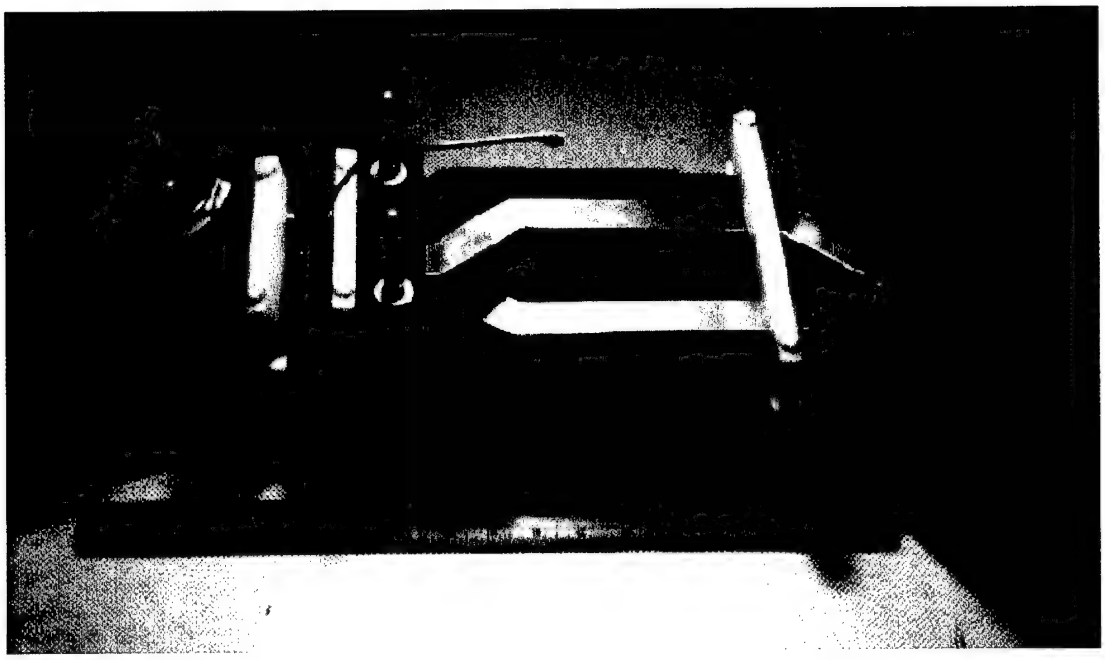

Figure 3. Photograph showing the 2-line A pulser (version 2) commutated by a photoconductive switch. Blumleins with line impedances of 100 Ω and line lengths of 25 cm are extended to the proximity of the stacking location, 23 cm from the switch assembly where the middle high voltage conductors are terminated. The lines then angled toward each other along with the dielectric for another 5 cm. At this point they are stacked directly on top of one another. The lines are connected in series for about 3.8 cm and the top and bottom plates are connected to a resistive load through a matched transmission line with a location for installing the capacitive probe. The resistive load is built from a stack of four 50 Ω, non-inductive carbon disc resistors. The top transmission line components of Blumleins are connected to the switch assembly while the bottom Blumlein conductors are placed about 6 cm from the switch assembly to allow installation of the capacitive probe used to measure launching waveforms at the switch. The pulser is capable of producing 100 kV, 2 ns output pulses with risetimes in the range 200-400 ps.

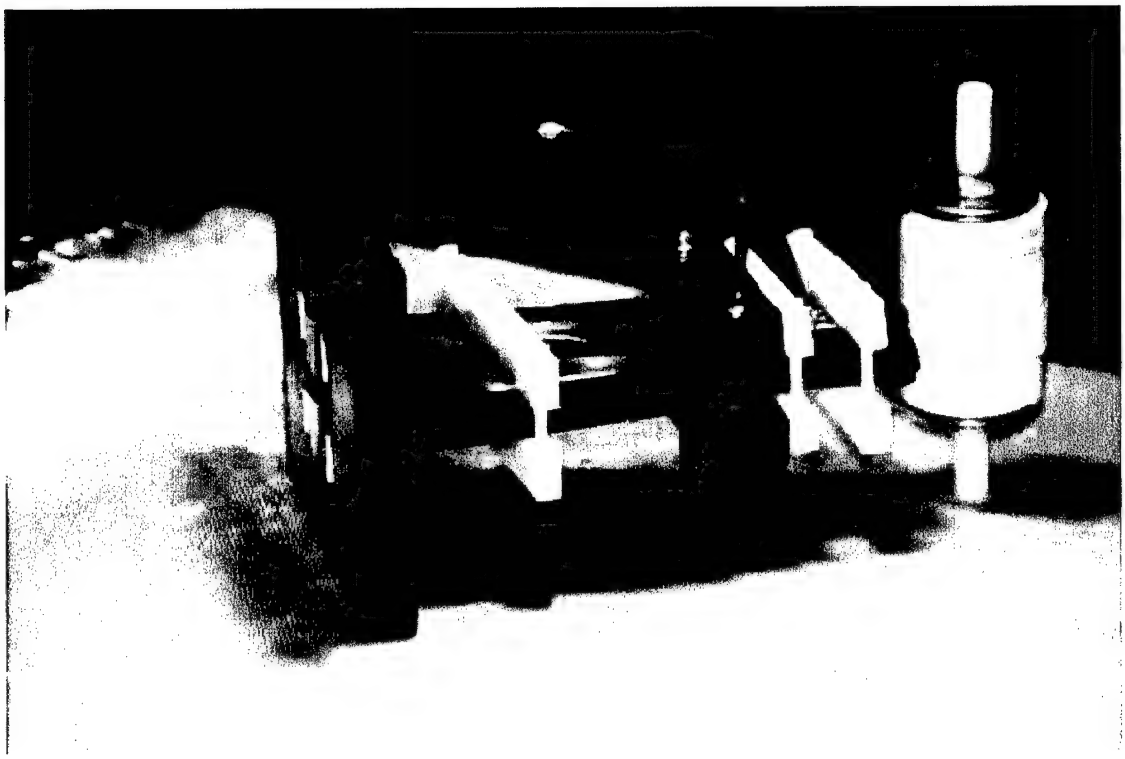

Figure 4. Photograph showing the 2-line B pulser commutated by a photoconductive switch. To exert less stress on the switch, we designed and constructed this device with shorter line lengths. As in the case of 2-line A device, the corresponding high voltage and ground copper plates for each of the Blumleins were connected together at the switch assembly. Blumleins with line impedances of 100 Ω and line lengths of 15 cm were extended to the proximity of the stacking location, 12.7 cm from the switch assembly where the middle high voltage conductor was terminated. The lines then angled toward each other along with the dielectric for another 5 cm. At this point they were stacked directly on top of one another. The lines were connected in series for about 3.8 cm and the top and bottom plates were connected to a resistive load built from a stack of four 50 Ω, non-inductive carbon disc resistors. Bottom Blumlein conductors were placed about 6 cm from the switch assembly to allow installation of the capacitive probe used to measure launching waveforms at the switch. The pulser is capable of producing 1 ns output pulses with risetimes faster than 300 ps.

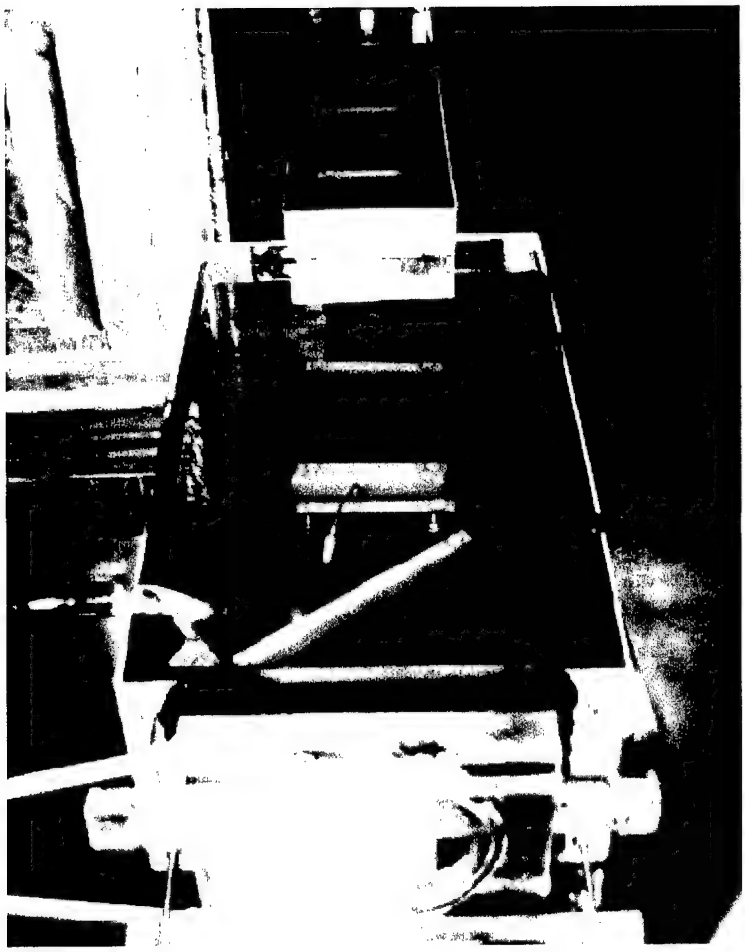

Figure 5. Photograph showing the 2-line B pulser with an extended 80 cm transmission line commutated by a photoconductive switch. This is done in order to delay any mismatched reflections beyond the measurement window. The resistive dummy load was transferred to the end of this line, as shown. The pulser is capable of producing 1 ns output pulses with risetimes better than 300 ps.

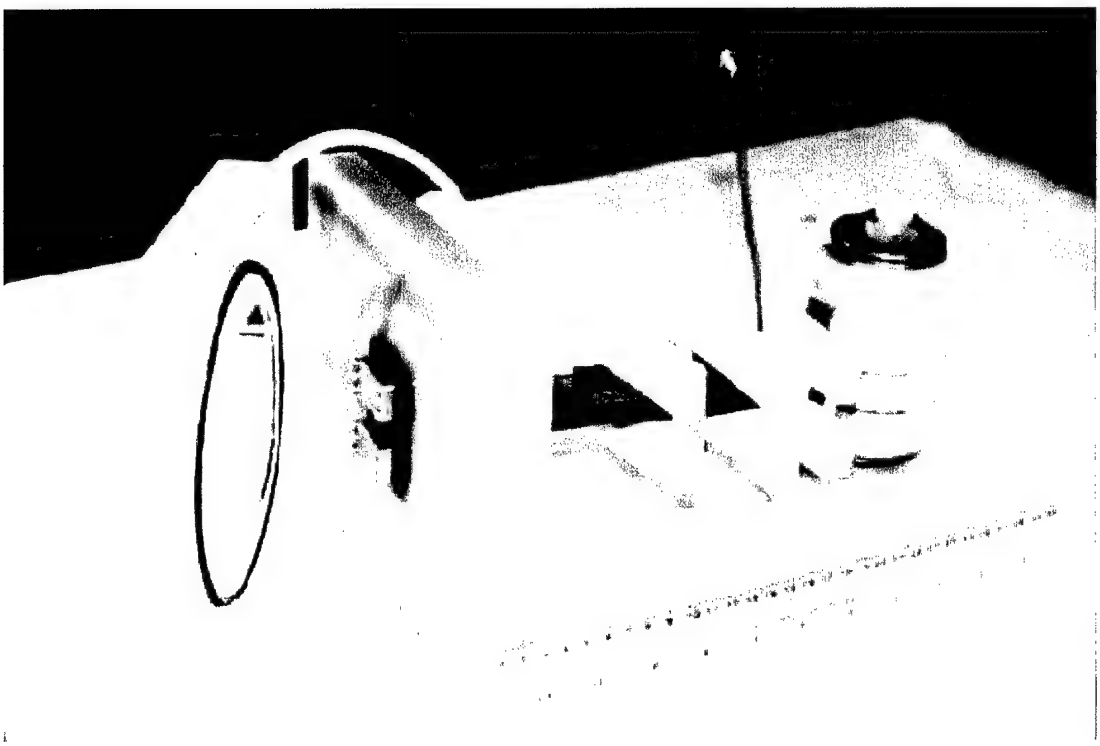

Figure 6. Photograph showing the 2-line B pulser (version 2) commutated by a photoconductive switch. This device is constructed in a low profile geometry. The corresponding high voltage and ground copper plates (1.27 cm wide) for each of the Blumleins are connected together and extended 1.5 cm for connection to the switch assembly. Blumleins with an impedance of 100 Ω are continued to the proximity of the stacking location, 11 cm from the switch electrodes, where the center, high-voltage conductor is terminated. The lines are angled toward each other along with the dielectric for another 2.5 cm. At this point, they are stacked directly on top of one another. The lines are joined in series for about 2.5 cm, and the top and bottom plates are connected to a matched resistive load built from a stack of four 50-Ω, non-inductive carbon disc resistors. The switch assembly is modified to provide a low-inductance connection to the pulse forming line. The base of the assembly contains two copper electrodes cast in a G-10 plastic plate. The pulse forming line is connected to the back of the electrodes with screws. The switch wafer is held in place by means of two copper holders screwed to the electrodes. The pressure cover was made from plexiglas and contained a chamber, into which the electrodes fit. The pulser is capable of producing 1.5 ns output pulses with risetimes on the order of 200 ps.

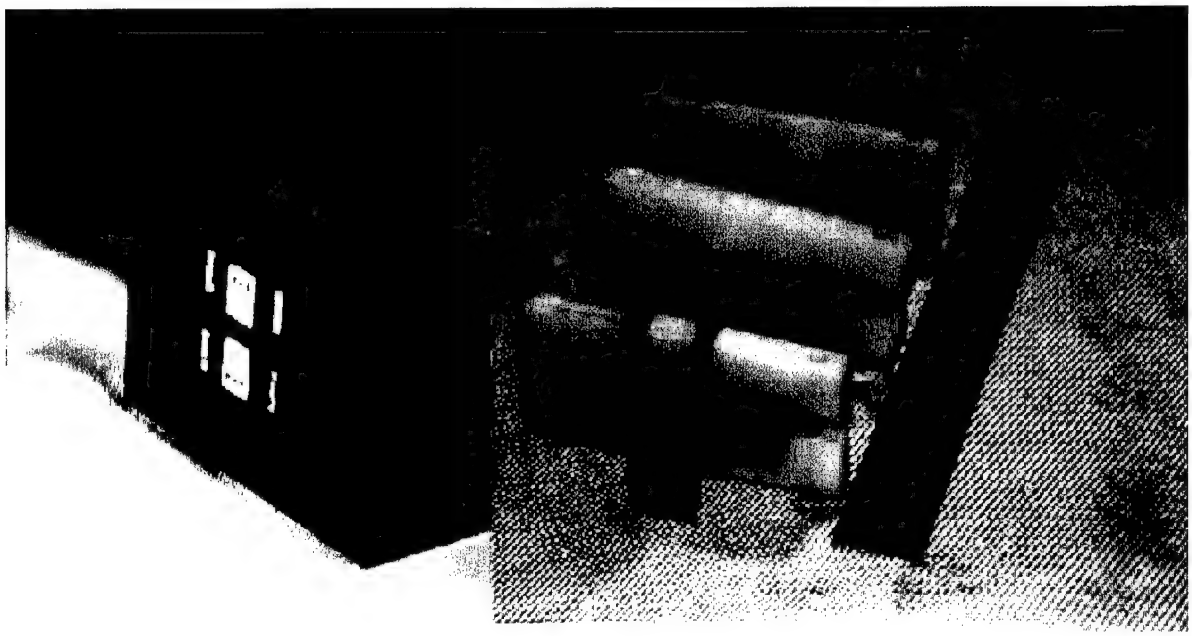

Figure 7. Photograph showing the 2-line C pulser commutated by a photoconductive switch. In this version, Blumleins with conductor widths of 1.27 cm are directly connected to the switch electrodes 2.54 cm wide before casting as shown. Two Blumleins with impedances of 100 Ω are extended to the proximity of the stacking location, 10 cm from the electrode assembly where the middle high voltage conductor is terminated. The lines then angle toward each other along with the dielectric for another 5 cm where they are stacked directly on top of one another. The lines then are connected in series about 1.27 cm and the top and bottom plates are connected to a resistive load built from a stack of four, 50 Ω non-inductive carbon disc resistors. Bottom Blumlein conductors are positioned about 1.27 cm from the electrode assembly. Blumleins together with the electrode assembly are potted in place as shown. This device produces 1 ns output pulses with risetimes better than 200 ps.

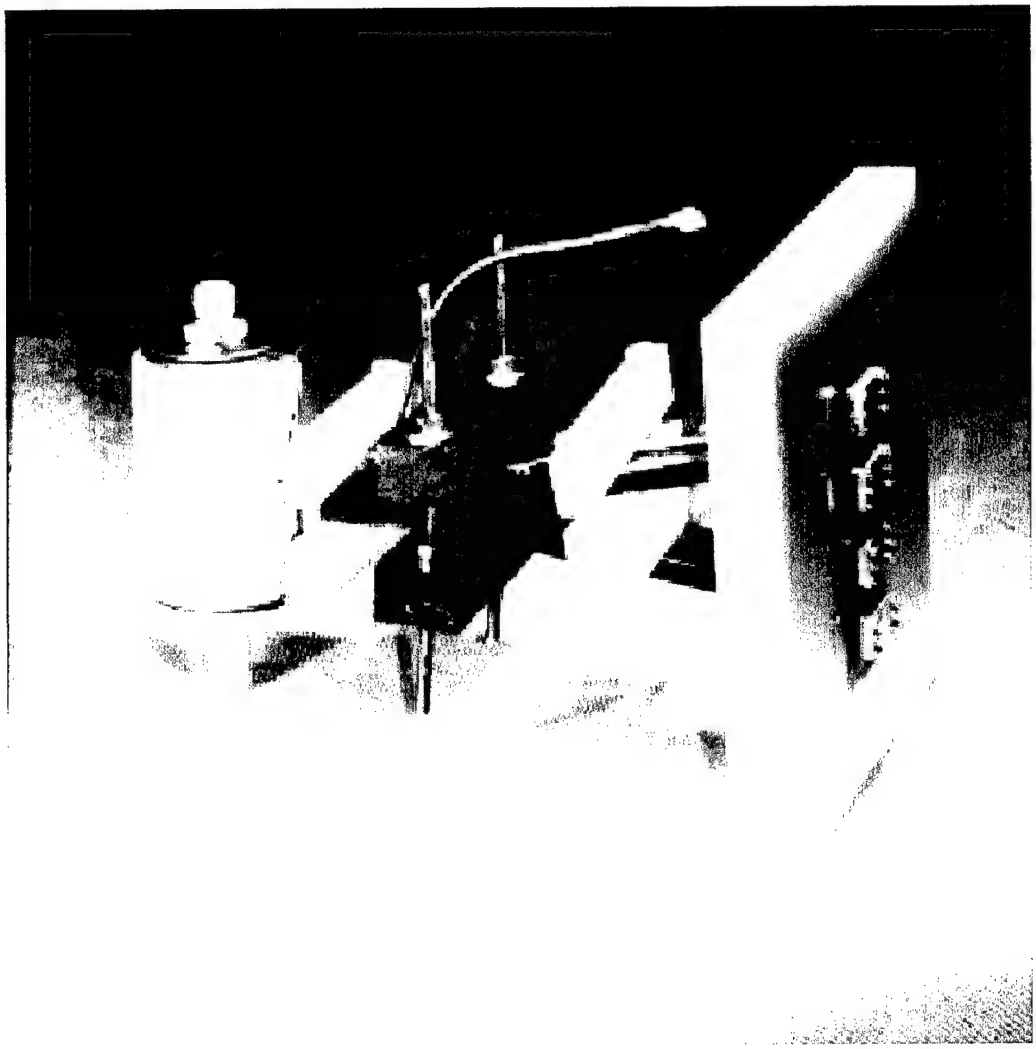

Figure 8. Photograph showing the 4-line pulser (version 1) commutated by two photoconductive switches. The pulser is designed and constructed by combining two units of 2-line B (version 2). The commutation assembly is reconfigured to contain two electrode sets as shown. The pulse forming lines in each 2-line unit are bent in a manner to bring the stacking sections to the same location one above the other. The units are joined in series and the top and bottom plates are connected to a resistive load built from a stack of four 100 Ω, non-inductive carbon disc resistors. This pulser is synchronously commutated by two GaAs photoconductive switches and is capable of producing 1.5 ns output pulses with risetimes in the range of 300-700 ps.

2. Laser Diode Activation

Initially, two types of single-heterojunction gallium arsenide injection laser diode arrays, the LD-215 and the LD-220, were acquired from Laser Diode, Inc. to activate the GaAs photoconductive switches in our pulsers. The LD-215 diode is capable of emitting a maximum of 120 W peak power and has 12 diode elements which are configured in a straight line. The LD-220, on the other hand, can emit a maximum of 240 W from 24 diode elements positioned in two parallel straight lines. Both lasers emit peak intensities at a wavelength of 904 nm.

To drive these lasers, two types of driver modules were purchased from Directed Energy, Inc (DEI). These were built in configuration LDM150-201N09, and were capable of producing 40-A current pulses with durations of 10 and 40 ns for the laser diode array. Both modules were placed in a RF shielded container and proper electrical connections were provided in order to trigger and power the drivers as well as monitor the laser diode current pulse. Measurement of the output from these laser diode arrays have been performed and excellent pulse stability, on the order of 20 ps, and a pulse risetime better than 700 ps were obtained. This is encouraging because the laser diode was powered with the low cost LDM150-201N09 laser diode driver commercially available from DEI.

We observed that there were no appreciable differences in the switch activation when either one of the laser pulse durations was used. For example, the LD-220 laser diode activated the device with laser pulse energies and durations of about 8.8 μJ or 2.2 μJ and 40 ns or 10 ns, respectively. It appeared that the avalanche was initiated and sustained as soon as the activating photon flux reached the threshold necessary for switch closure. The remaining photons in the pulse did not contribute to the process afterward. The importance of these results was that laser

pulse durations even shorter than 10 ns may be able to activate the switch, as long as the peak power stays the same [8].

Recently, a relatively low power laser diode array, POS 904, acquired from Power Spectra, Inc., was used to trigger GaAs photoconductive switches. The POS 904 can emit a maximum of 50 W peak power at a wavelength of 904 nm. It has 3 diode elements that are configured in a straight line. In operation, this laser emitted a peak power of about 46.5 W in 6.4 ns (FWHM), corresponding to a laser pulse energy of about 300 nJ. Trigger laser photons are delivered to the switch by collimating and focusing the laser beams in straight lines across the switch from the cathode to the anode.

3. Improvements to Charging Pulse Compression Module (CPC)

During our earlier work, we introduced a novel charging system for the short pulse devices commutated by photoconductive switches [12]. The Charging Pulse Compression (CPC) module conditions the output of the pulse charging power supply so that the lines and the photoconductive switch in the final module are subjected to a high voltage for about 80 ns. The fast charging capability of the CPC module significantly improves the GaAs switch lifetime. It should be noted that the CPC was originally designed to charge a variety of short-pulse final modules with different system capacitances. It provides more energy than needed to charge a stacked Blumlein such as 2-line B (version 2) with a relatively small capacitance. For such systems, a combination of limiting resistors and inductors has been used in the charging circuit to compensate. However, for a particular stacked Blumlein, the CPC can be easily modified to deliver proper energy for charging.

During this research, we modified the CPC to provide low energy charging of the 2-line B (version 2) in 20 ns. The design and construction of the CPC is similar to the single Blumlein pulse generators developed at UTD. It consists of two subassemblies: (1) a single Blumlein pulse forming line, and (2) a commutation system capable of operation at high repetition rates.

Before this modification, the CPC had a Blumlein that consisted of three conductor plates, 2.5-m long, separated by 1.65-mm-thick laminated Kapton insulators. The switching and storage capacitances of the Blumlein were 4.2 nF each. The line had a smooth taper, which decreased the width of the line from 20 cm at the thyratron to 10 cm at the load. In this work modifications were performed mainly to the Blumlein pulse forming line. Dielectric boards of G-10 3.3-mm-thick were added to the existing Kapton boards to decrease the storage and switching capacitances of the Blumlein to 2 nF each. Figure 9 shows a photograph of the CPC's Blumlein during assembly.

The Blumlein middle conductor is placed on the top of G-10 and Kapton dielectric insulators as shown in Fig. 9. These boards separate the bottom conductor (not shown) from the middle conductor, forming the storage capacitance. The switching capacitance is formed by placing another set of dielectric board and a top conductor on this structure. The line taper was also modified to decrease the width of the line from 20 cm at the thyratron to 2.5 cm at the load. This was done to provide better match for charging the 2-line device. Photograph of the assembled CPC module is shown in Fig. 10.

In operation, the modified CPC was resonantly charged with a pulse power supply capable of operation in the range of 3-75 kV and repetition rates of 1-1000 Hz. The middle conductor was charged to a positive high voltage and commutation was effected by a thyratron mounted in a grounded cathode configuration.

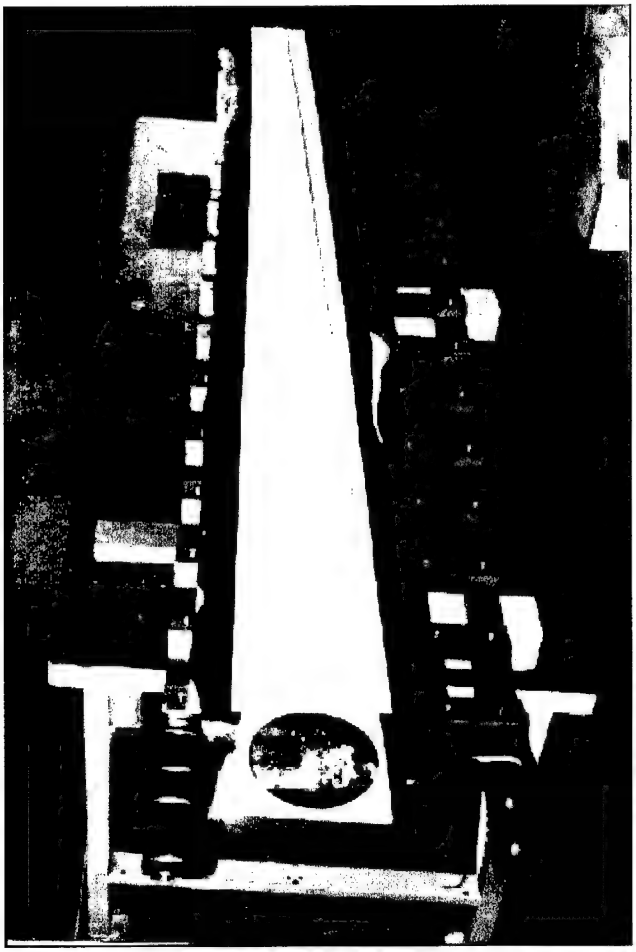

Figure 9. Photograph showing the CPC module during assembly.

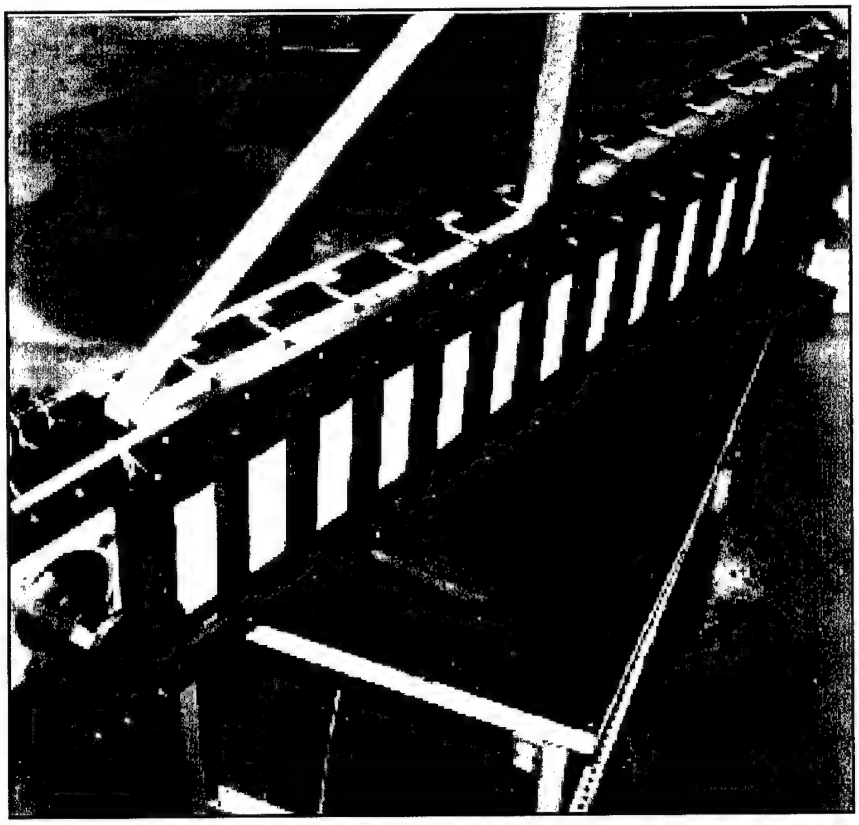

Figure 10. Photograph showing the assembled CPC module.

The output from this intermediate pulser was used to charge a stacked Blumlein prototype pulse. Figure 11 shows a charging profile obtained without commuting the photoconductive switch. It should be noted that the modification to CPC has reduced charging time for this particular device from 80 ns to 20 ns as seen in Fig. 11. This is expected to significantly improve lifetime of photoconductive switch used to commute the pulser.

4. Pulser Operation

To prepare for operation, the photoconductively switched pulser and the charging pulse compression (CPC) module were placed in separate RF shielded containers. The CPC module was resonantly charged using our conventional pulse power supply. Synchronization between various components in the system was maintained through a series of three timing pulses generated by a master oscillator. The first, or the instant pulse, triggers the glass thyratron in the power supply and started the charging cycle for the CPC module. After a delay determined by the charging time of the CPC device, a second pulse triggered the thyratron in the CPC and produced short charging pulses for the main pulser. The photoconductively-switched pulser was fully charged in about 20-80 ns, after which a third pulse triggered the laser diode array system and provided activation photons for the GaAs photoconductive switch. A schematic drawing of the power supply, CPC module and laser diode along with the timing circuit is shown in Fig. 12.

Currently, commutation of the photoconductively-switched stacked Blumlein is successfully achieved with a switching voltage in the range of 40-60 kV and laser pulse energies as low as 300 nJ. Examination of output waveforms indicates risetime better than 300 ps. A typical output voltage generated by the 2-line C prototype is presented in Fig. 13. The peak value corresponds to a voltage gain of about 1.8 that is consistent with our earlier results for the 2-line devices.

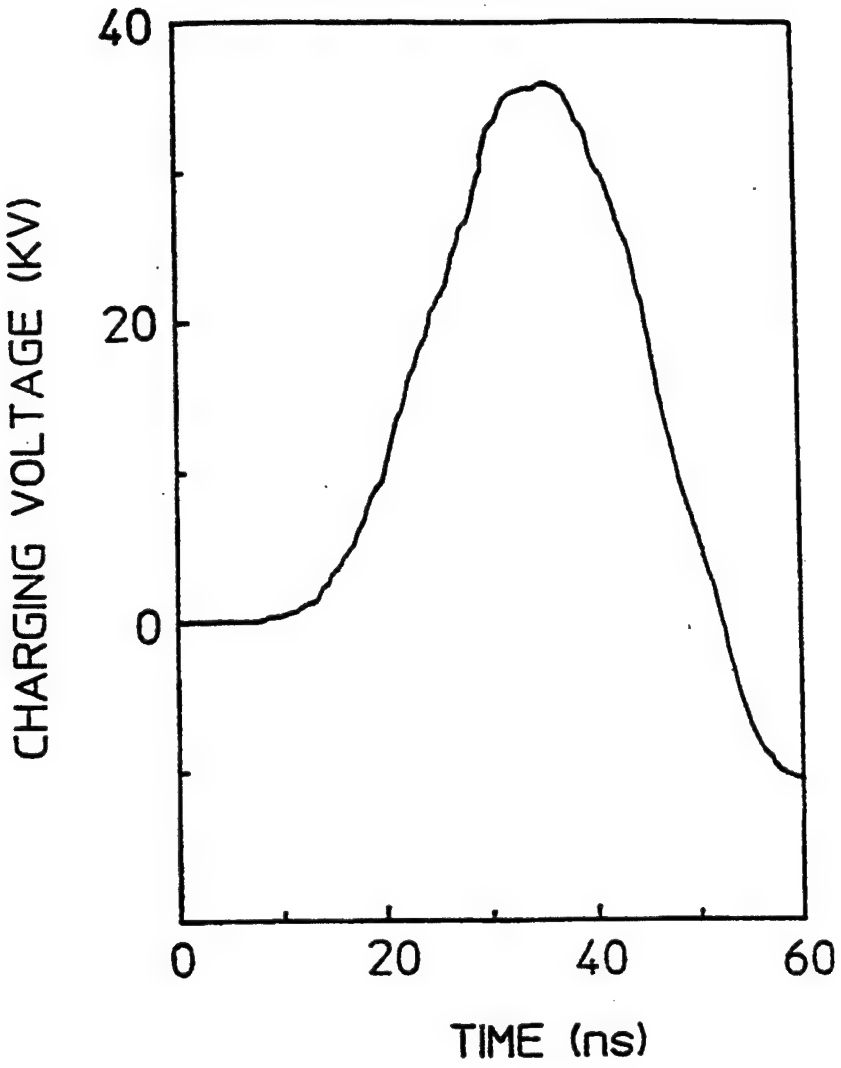

Figure 11. A voltage waveform generated by the modified CPC module charging the 2-line B pulser (version 2).

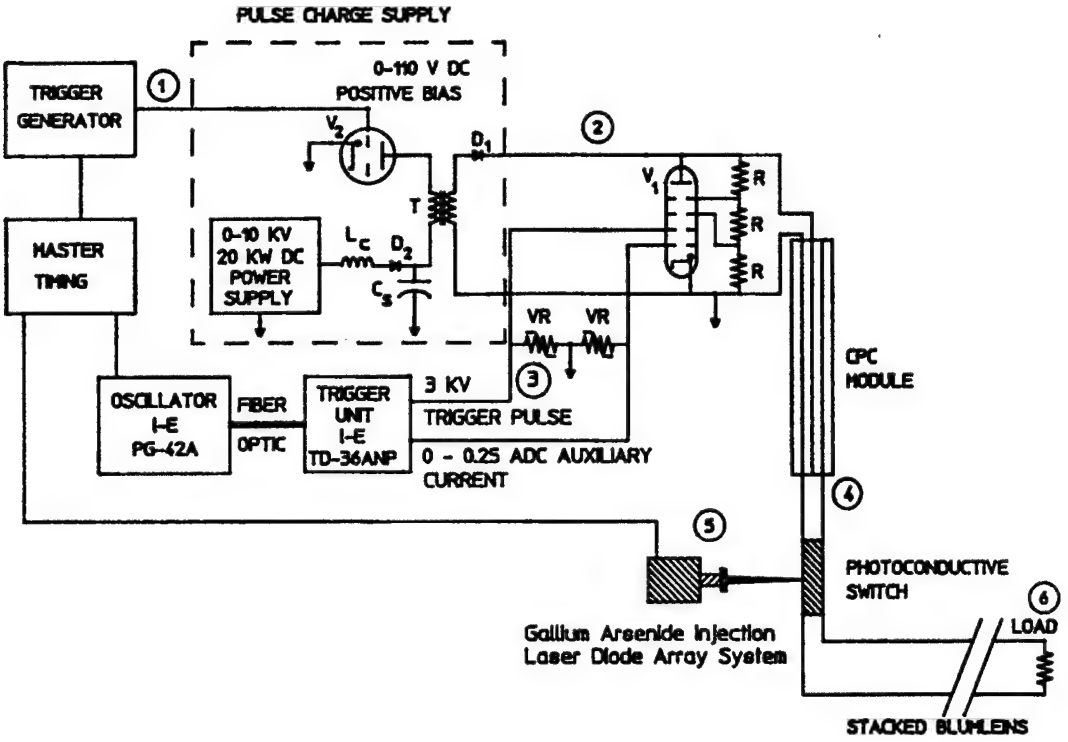

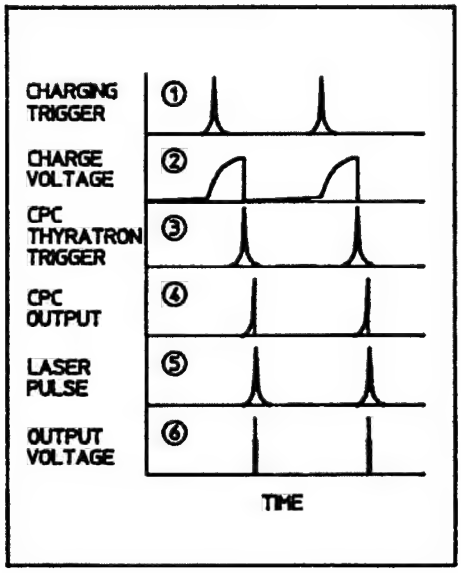

V_1 - Grounded cathode EG&G 5353 thyratron

V_2 - Positive grid EEV FX2525 thyratron

T - High voltage pulse transformer

R - High voltage 10 MΩ resistor

VR - High voltage varistor assemblies

D_1, D_2 - Charging diodes

C_S - Storage capacitor

L_c - Charging inductor

Figure 12. Schematic representation of the pulse power supply, CPC intermediate module and the laser diode assembly used to commutate the stacked Blumlein pulsers.

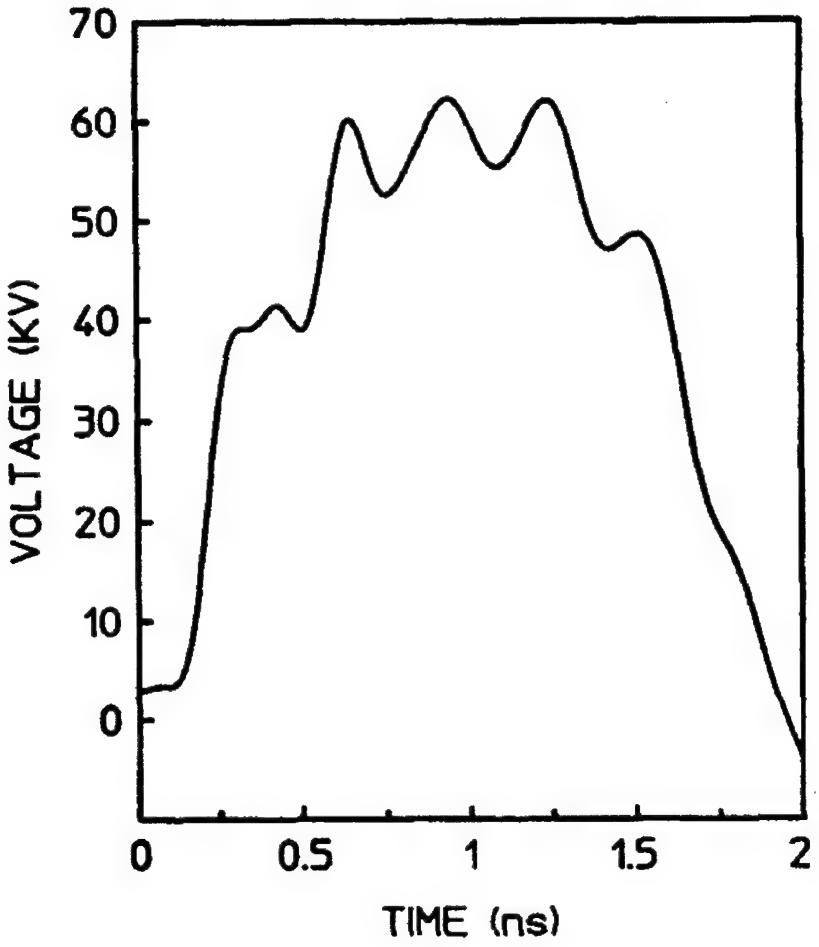

Figure 13. Voltage waveform obtained at the stack of the 2-line C pulser by commuting the device with a GaAs switch in the avalanche mode. This particular waveform corresponded to a charging voltage of 50 kV. Switch is activated by LD-220 laser diode array.

5. True Field Probing of the Waveforms

Capacitive sensors have been used to measure fast voltage transients in a variety of pulsed power systems. However, they are sensitive to stray charges and are difficult to calibrate, especially where measurements of high-voltage transients with frequency components of hundreds of megahertz is attempted and high level of electromagnetic noise in the experimental area exists. Furthermore, the sensor's time constants should be long enough so they act as voltage dividers with output signals proportional to the transmission line voltage pulse. To probe sub-nanosecond risetimes expected of waveforms generated by our pulsers, a capacitive probe has been used. It is self-integrating in the sub-nanosecond time regime. This probe has a simple geometry as shown schematically in Fig. 14. Prior to use of this particular probe we constructed and used capacitive probes with different geometries and installation procedures in order to study the response and increase their integrating capacitances.

For these experiments, we elected the 2-line B pulser (version 2) with the resistive load built from a stack of four 50-Ω, non-inductive carbon disc resistors as shown in Fig. 6. We believe that, at this stage of development, the placement of a dummy resistive load is sufficient for proper characterization of our devices within combined uncertainty of less than 10%.

We commutated the 2-line pulser with GaAs switch in the avalanche mode with the aid of the LD-220 laser diode, as described earlier in this report. Figure 15(a) plots the output voltage for the resistive loading mode of operation. The reasonable match seen in this figure demonstrates the proper determination of the device Blumlein line impedance of 100 Ω. We also operated the 2-line pulser in the open circuit mode with no load connected to the stack. The output voltage pulse generated is presented in Fig. 15(b). Charging voltage of 40 kV was used to obtain these waveforms.

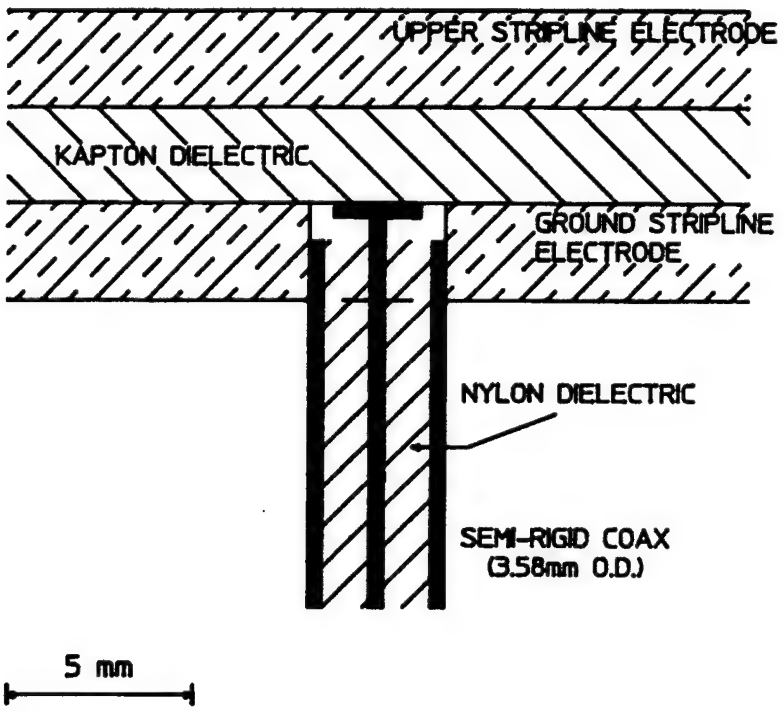

Figure 14. Schematic drawing of the capacitive voltage probe used in this work.

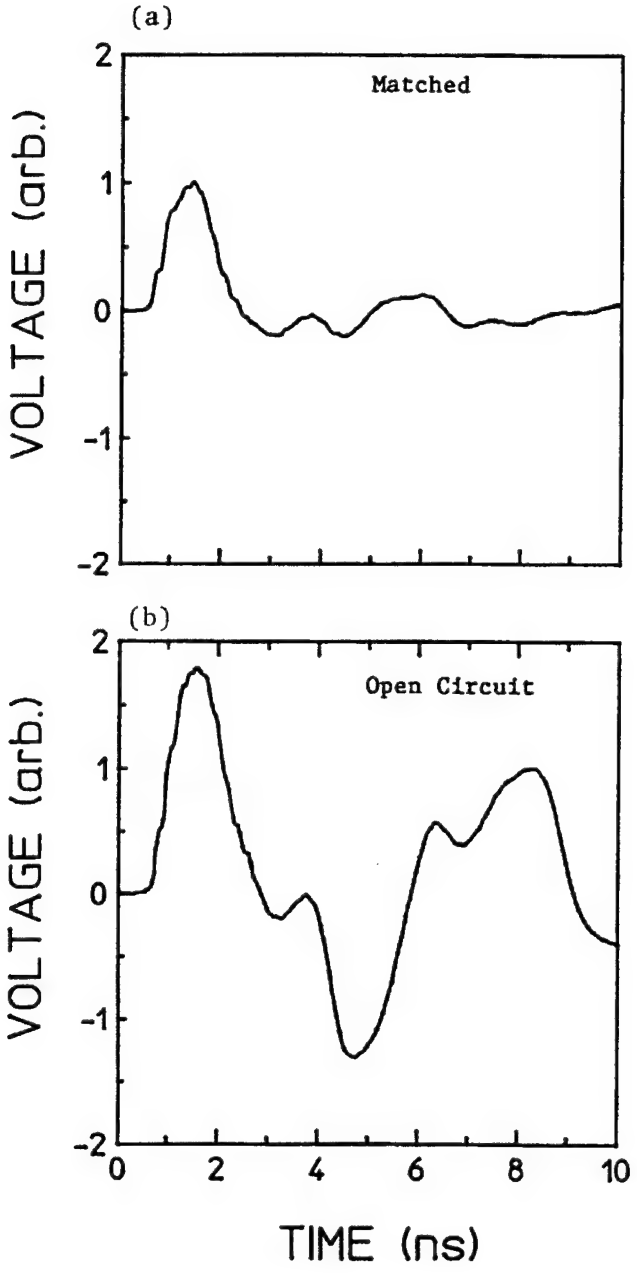

Figure 15. Output voltage waveforms obtained by operating the 2-line B (version 2) pulser with (a) matched resistive load (b) open circuit with no load. Device was operated with a charging voltage of 40 kV.

The voltage amplitude of Fig. 15(b) approaches twice voltage amplitude of Fig. 15(a) that was obtained with a matched load. Please note that the Figs. 15(a) and 15(b) were plotted on a same relative scale. This further demonstrated the proper match with the resistive dummy load and the accurate determination of Blumlein impedances for our pulsers. In the case of Fig. 15(a), the pulse width corresponds to the two way transit time of Blumleins in the 2-line device indicating the capacitive voltage probe was an integrating probe in this time regime.

To investigate this further, we increased the output pulse duration available from the 2-line B pulser (version 2). This was done by increasing the length of Blumleins by about 50%. Blumleins with impedances of about 100 Ω were continued to the proximity of the stacking location, 17 cm from the switch electrodes, where the center, high-voltage conductor was terminated. Then as for the original device, the lines angled toward each other with the dielectric for another 2.5 cm. At this point, they were stacked directly on top of one another. The lines were joined in series for about 2.5 cm, and the top and bottom plates were connected to a matched resistive load through a very short transmission line with a location for installing the capacitive probe. The pulse forming sections for the original and modified 2-line pulser are shown in the photograph of Fig. 16 for reference.

Figures 17(a) and 17(b) plot on a same relative scale voltage pulses generated by the 2-line pulsers with pulse forming lines shown in Fig. 16. Charging voltage of 40 kV was used to obtain these waveforms. Comparison of Figs. 17(a) and 17(b) indicates that the pulse durations are proportional to Blumlein lengths, corresponding approximately to the two-way transit times of Blumleins. These investigations demonstrated the self-integrating nature of our capacitive probe in the time regimes of these studies. In addition, the modifications made to the 2-line B pulser (version 2) increased output pulse durations to about 2.5 ns as seen in Fig. 17(b)

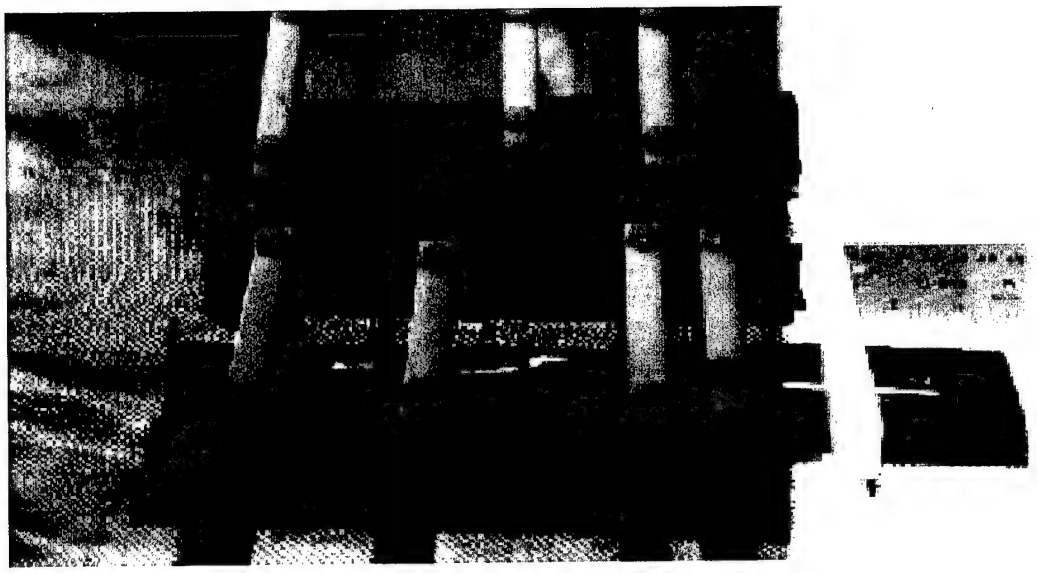

Figure 16. Photograph showing the original and modified pulse forming assemblies for the 2-line B (version 2) pulser characterized in this work.

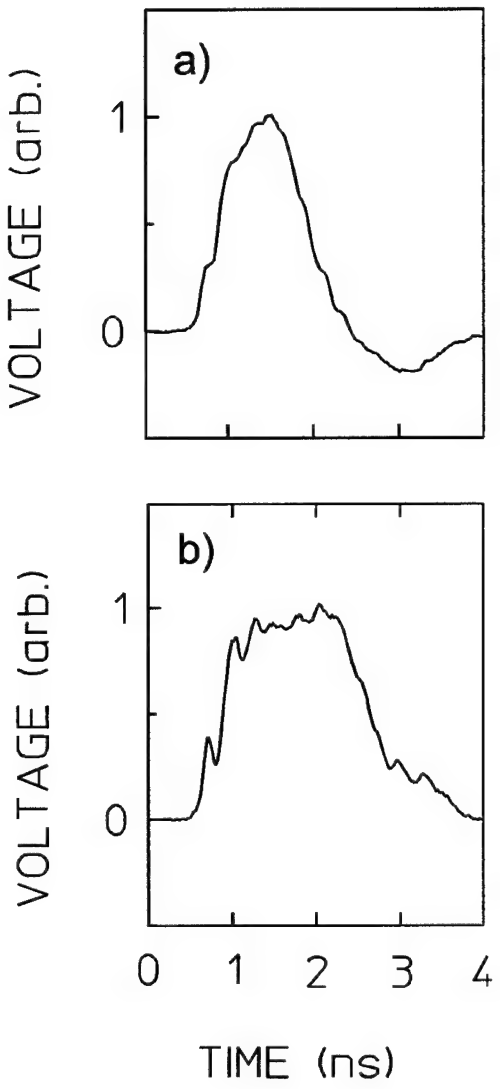

Figure 17. Output voltage waveforms obtained by operating the 2-line B (version 2) pulser with Blumlein lengths of (a) 11 cm and (b) 17 cm. Device was operated with a charging voltage of 40 kV.

SWITCH LIFETIME CONSIDERATIONS AND STUDIES

1. Avalanche Initiations and Current Filamentation

During the avalanche-mode switching of a device such as HPM pulser, the current is concentrated in filaments that extend from the cathode to the anode across the insulating region of the GaAs switch in a lateral configuration [13]. Carrier recombination results in the emission of characteristic band gap photons in the near infrared region, which can be seen by an infrared viewer.

We have observed these effects in experiments where laser diodes provided trigger photons for the avalanche commutation of the stacked Blumlein pulsers. As soon as the avalanche is initiated, a single filament can be observed with an infrared viewer, which approximately follows the collimated laser beam that was focused in a line from the cathode to the anode. The middle plot in Fig. 18 shows this behavior, which occurs the majority of time during switching. Multiple branching from the avalanche initiation point has also been observed but with much less probability as seen in Fig.18. Filamentary currents with densities of several MA/cm^2 with diameters of 15-300 μm passing through a narrow channel can cause switch damage, especially at the contacts points. A greater number of filaments during each cycle of commutation reduce the stress on the switch, thereby increasing its lifetime.

During this research program, a substantial amount of effort was directed to study and implement the broadening of the current channels in the avalanche photoconductive switch in order to improve lifetime and increase switching peak power. This was performed by two approaches. The first was control of laser diode beam delivery to the switch and switch contact improvements. The second approach was the study of the feasibility of the use of amorphic diamond as a photoconductive switch cathode enhancement in conjunction with the stacked Blumlein pulse generators.

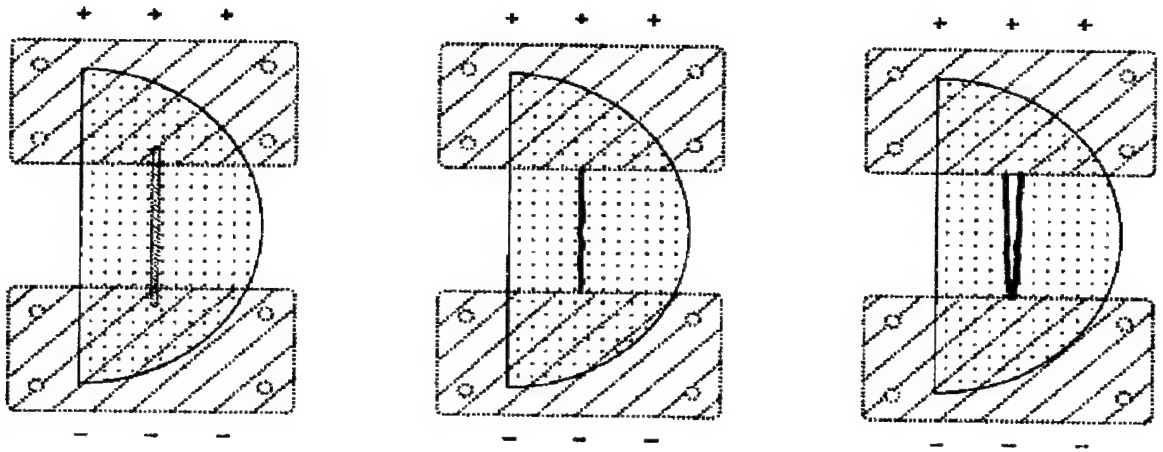

Figure 18. Schematic diagrams of a laser diode beam focused on the switch in one line, and current filamentation seen with an infrared viewer.

2. Switch Contact Deposition

It is clear that the switch contact plays an important role in reliable operation of any pulser with photoconductive switches. However, innovations in stacked Blumlein design, fabrication and charging schemes have resulted in generation of high power nanosecond waveform with reasonable pulse stability and switch lifetimes, even when the switch contacts to electrodes were made by mechanical pressure alone.

In order to improve the operation further, in this work, we prepared a high vacuum system for metal contact evaporation. Figure 19 reproduces the photographs of the vacuum chamber and related equipments for reference. Highly adhesive metal coatings were deposited on switch materials. Figure 20 shows a photograph of copper and germanium coatings 0.2-mm thick each on GaAs substrates. The coating adhesions were able to pass tape tests performed according to military specification MIL-C-00675.

3. Amorphic Diamond Coating of GaAs Switches – Concept

It has been determined that amorphic diamond emits electrons at high current densities when immersed in modest electric field strengths. Therefore it is anticipated that by depositing films of amorphic diamond near the switch contacts, the number of carriers and avalanche sites may increase aiding the switch performance. In addition, damage to the switch at the contact points during commutation may be reduced, improving the switch lifetime. Figure 21 schematically presents the concept. In this figure, the GaAs switch is shown with the metal electrode contacts and a coating of amorphic diamond on and around the cathode electrode.

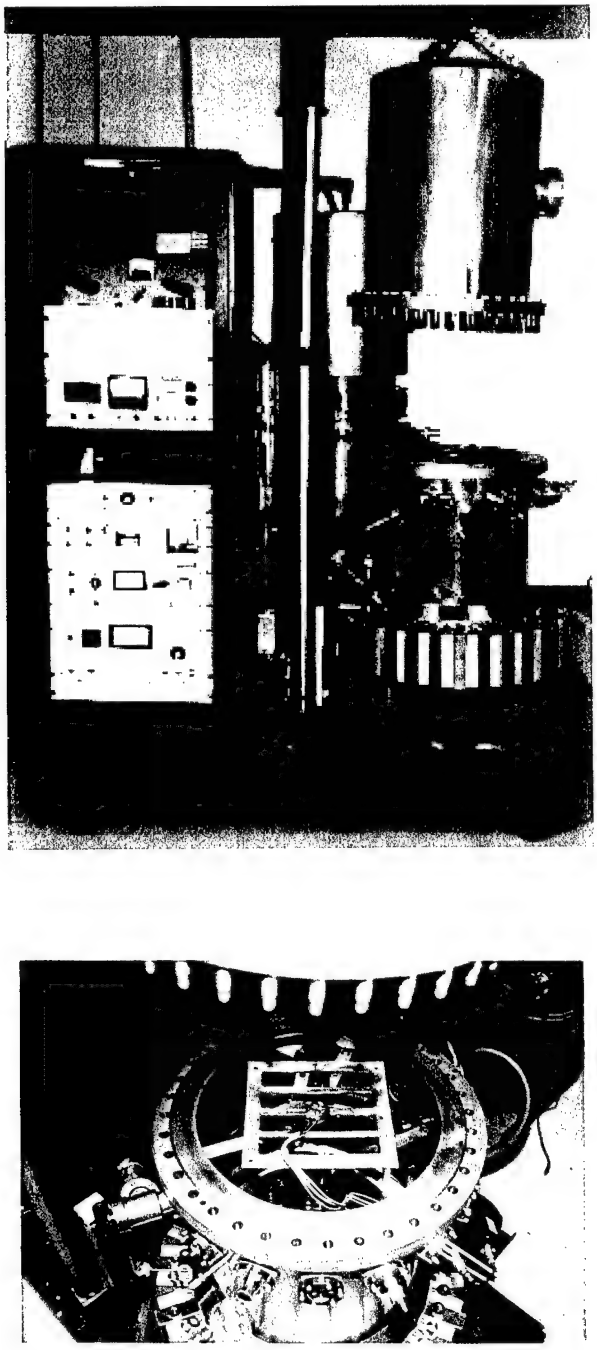

Figure 19. Photographs showing the vacuum chamber and related control units and equipments. A close-up view of the interior of the chamber with a crucible and a thickness monitor is also presented.

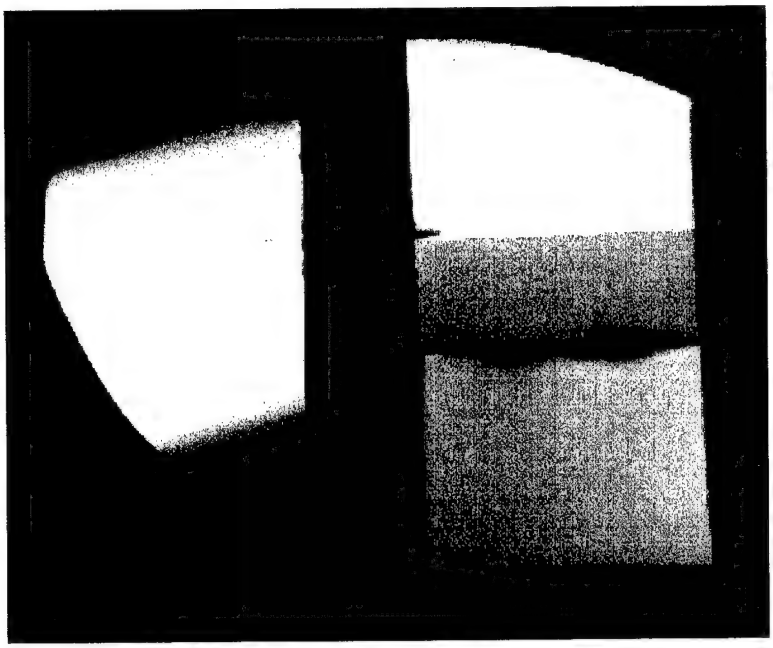

Figure 20. Photograph showing coatings of copper and germanium on a switch material.

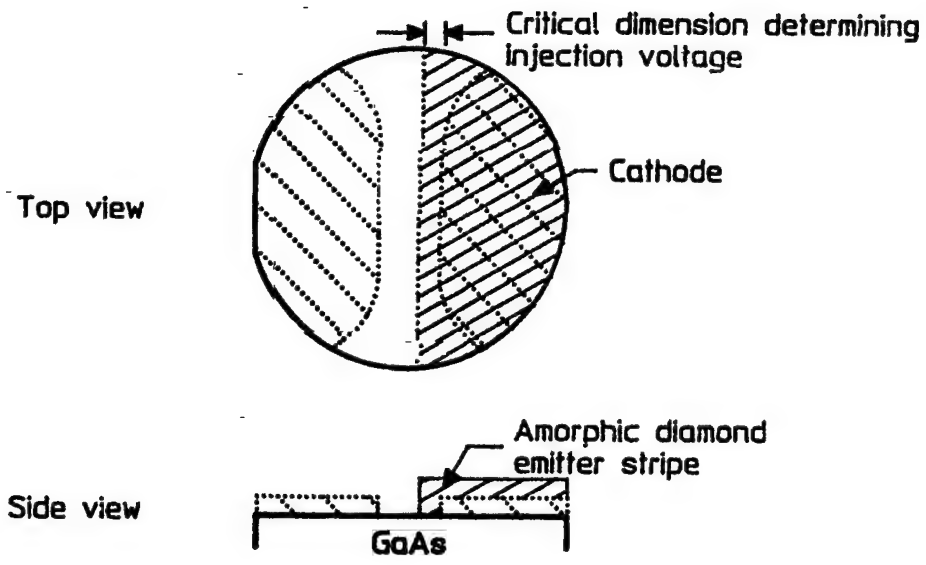

Figure 21. Schematic diagram of the concept for a GaAs photoconductive switch with pre-avalanche seeding from amorphic diamond photoemitter.

The vacuum system used to deposit our amorphic diamond has been modernized to be adequate for advanced studies. However, the working chamber had a fixture which was suitable for uniformly coating flat test substrates 25 mm in diameter. During this work we adopted the deposition system for uniformly coating GaAs wafers 50 mm in diameter. Highly adhesive coating of amorphic diamond on GaAs switches were obtained which were able to pass harsh tape tests performed according military specification MIL-C-00675. Strips of amorphic diamond coatings were deposited on GaAs switches at either cathode locations or at both cathode and anode locations as shown in photograph of Fig. 22. We also prepared fixtures to enable the deposit of the amorphic diamond with a gradient of thickness on GaAs switches. Coating thickness change may be required to distribute electric fields more uniformly around the switch assembly avoiding possible arcs and improving switch lifetime. Figure 23 shows a photograph of a switch coated with amorphic diamond around the cathode contact. The diamond coating was deposited over and around the cathode ohmic contact as schematically shown in Fig. 21.

The junction between an intrinsic GaAs semiconductor and a metal contact produces a Schottky barrier that impedes carrier reinjection and results in an effective carrier lifetime that is less than the bulk recombination time. This effect has been countered by fabricating heavily doped ohmic contacts to reduce the thickness of the Schottky barrier and permit efficient tunneling. However, the large carrier density and the conduction electric field generate very large fields near the contact to promote carrier injection and to form an equilibrium electric field. The large electric fields generated by charge movements cause local surface flashovers and reduce the switch lifetime. It is anticipated that application of thin film amorphic diamond as shown in Figs. 22 and 23 will also aid efficient tunneling of carriers while protecting the switch from localized damage.

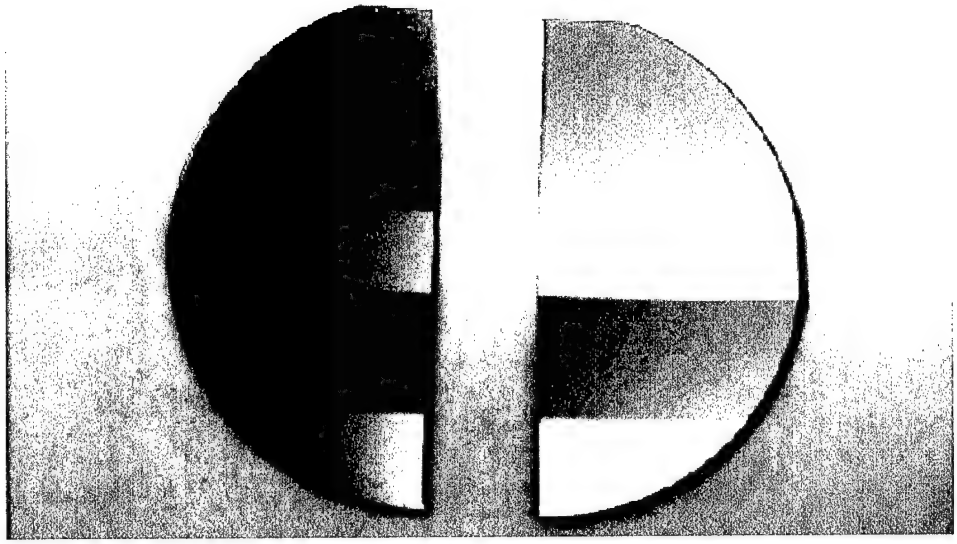

Figure 22. Photograph showing two GaAs switches with strips of amorphic diamond coatings.

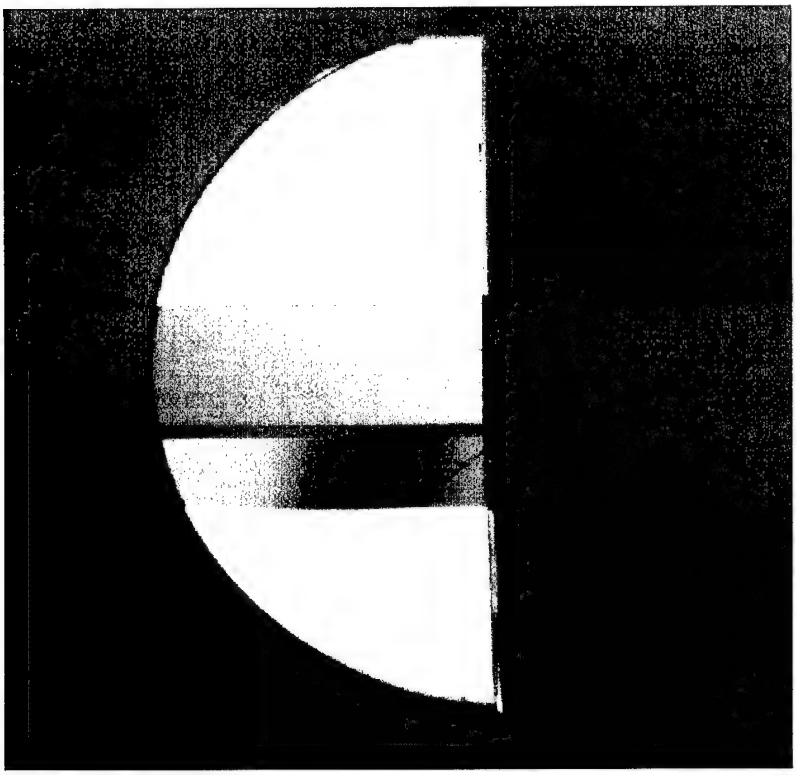

Figure 23. Photograph showing a GaAs switch with metal contacts coated with a strip of amorphic diamond near the cathode. Thickness gradient of diamond coating is seen by the optical interference pattern indicating thicker coating at the straight edge of the switch.

4. Switch Lifetime Studies with Metal Contacts

We have implemented several switch mounting configurations in our commutation assembly which is schematically shown in Fig. 24. The base of the assembly contained two copper electrodes cast in a G-10 plastic plate. The pulse forming lines were connected to the back of electrodes with screws. For the sake of consistency, we used the 2-line B pulser (version 2) in our photoconductive switch lifetime studies.

Each switch was fabricated from one half of a semi-insulating LEC grown GaAs wafer with a diameter and thickness of 5 cm and 0.5 mm, respectively. It was held in place by means of two copper holders screwed to the electrodes as shown in photograph of Fig. 25. Activation of switch was implemented by collimating and focusing the LD-220 laser diode array beam in two straight lines across the switch gap from cathode to anode.

An isometric view of the switch/electrode configuration used in these studies is shown schematically in Fig. 26. Top copper electrode holders were connected to the base electrodes by means of several screws. In this way the photoconductive switch was held in place firmly by mechanical pressure. The switch longevity was tested with the GaAs switches fabricated either with no coating or with single or multilayer metal/diamond coatings as shown. Deposition of metal contacts and diamond thin films were performed on either one or both sides of the GaAs wafer. The switch/electrode configuration seen in Fig. 26 allowed current conduction to be directed only through top electrode holders or only through base electrode contacts with switch, by placing a layer of Kapton polyimide insulator between switch and base electrodes or between switch and top electrodes, respectively. In all the experiments described here, a switch voltage of 60 kV was used to commutate the 2-line B pulser (version 2) with the switch assembly shown in Figs. 25 and 26.

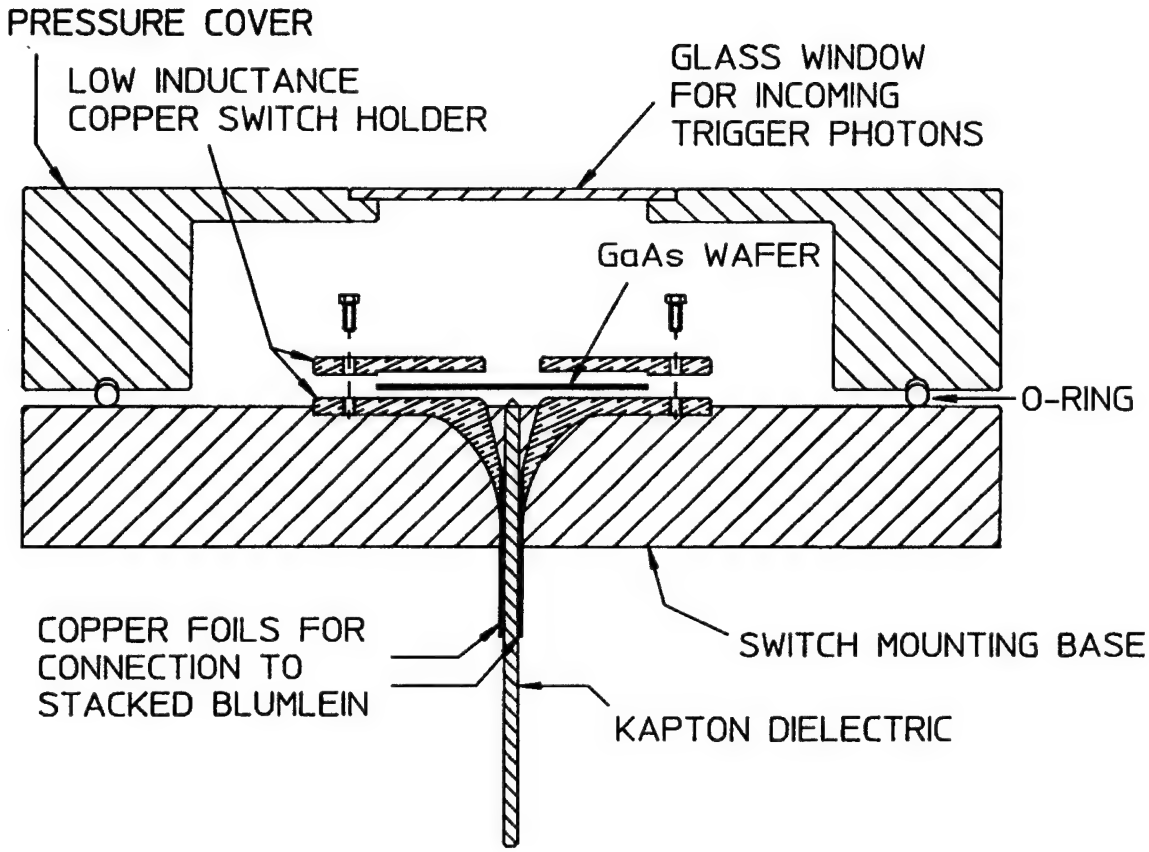

Figure 24. Schematic drawing of the cross-section of the switch assembly used in our photoconductively switched stacked Blumlein pulsers.

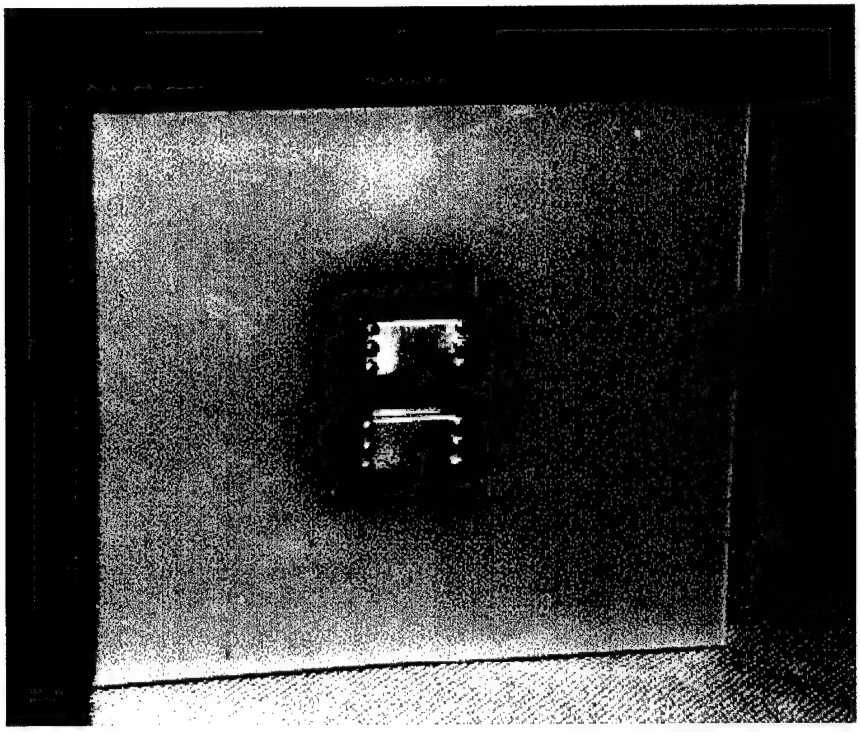

Figure 25. Photograph showing switch mounting configuration used in this study to hold a switch made of a half a GaAs wafer.

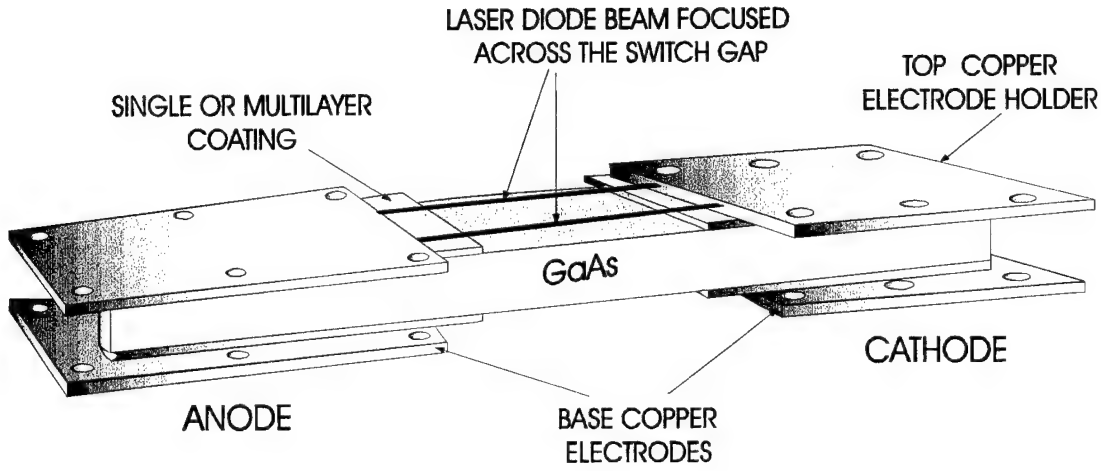

Figure 26. Schematic drawing of the switch/electrode configuration used in these switch lifetime studies.

It should be emphasized that the high currents passing through a narrow channel of a filament coinciding with the focused laser beam can cause switch damage at the switch / electrode contact points. To avoid severe damage at the contact areas a beam scanning system was used. It scanned the focused laser beam across the switch width and thereby the location of the current filament for each cycle of commutation was changed. This method improved switch longevity by distributing the damage across the switch width.

We began the tests by using a GaAs switch with a germanium contact 125 nm thick, deposited in house on both sides allowing a 10 mm switch gap. It was placed in the switch assembly shown in Fig. 26 in a way to leave a 1 mm distance between switch gap boundaries and copper electrodes. The switch commutated the pulser at 72 MW for 3×10^3 shots after which it was failed. The appearance of damage on both sides of the switch is shown schematically in Fig. 27. After several hundred cycles of commutation, dark regions at the limit of the copper plate electrodes appeared which eventually caused thermal run away at the switch gap surface and produced a switch crack.

It is interesting to note that there was no damage to the Ge contacts at the switch gap boundaries. This indicated that the thin layer of Ge was unable to support conduction of current laterally, as expected. Due to semiconductive nature of Ge, the skin depth was several millimeters at the frequency of this experiment and only conduction through the thickness of the Ge film was possible. This suggested that avalanche sites were created near contact areas. However, filamentary currents with very high densities passing through a narrow channel through thickness of Ge coating and into GaAs caused damage as characterized by dark regions shown in Fig. 27.

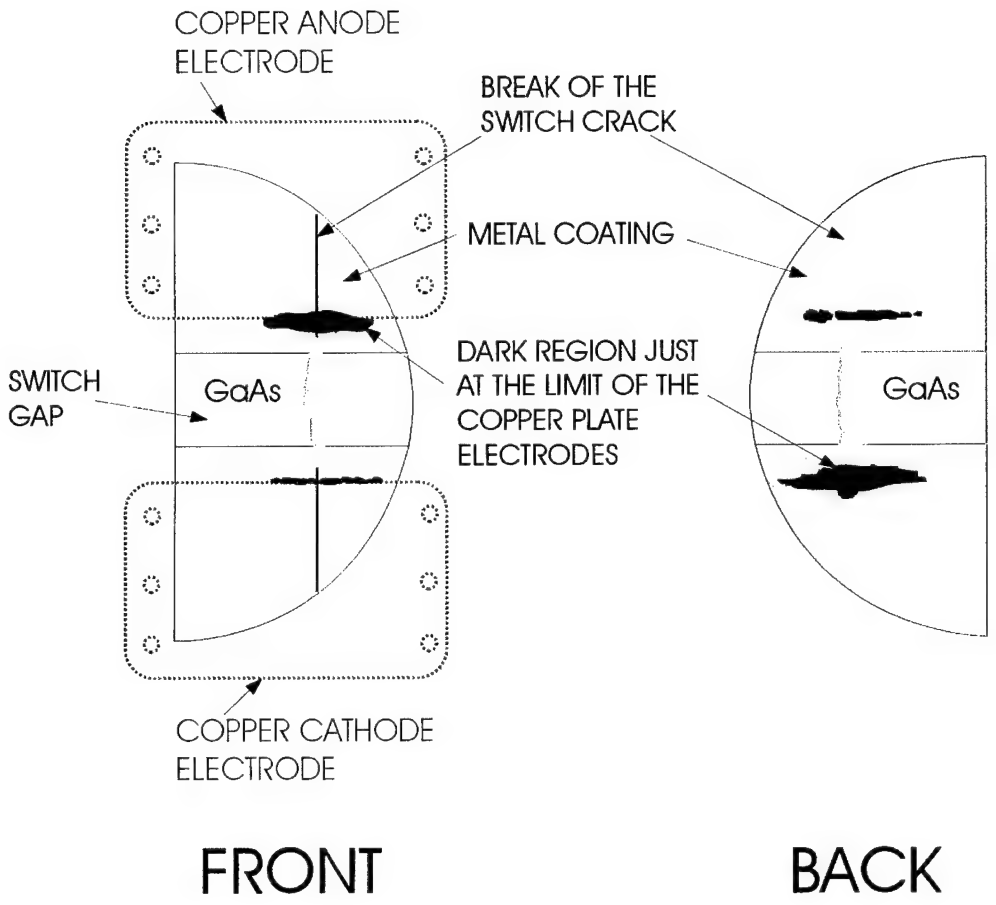

Figure 27. Schematic drawing of the appearance of damage on both sides of the switch used in these studies.

We increased the distance between switch gap boundaries and copper electrodes from 1 to 3 mm and repeated the experiment. No switching occurred because the carriers and pre-avalanche locations were far from the electrode contacts to allow current conduction through the thickness of the Ge coating and across 3 mm of bulk GaAs. This seemed to indicate that the avalanche processes were initiated very close to switch electrodes where the initial carriers had been generated by laser photon absorption. This suggested the importance of delivering activating laser photons to proximity of switch electrode contacts.

We observed damage on the front and the back of the switch at the copper electrode contacts as seen in Fig. 27. This seemed to indicate that the conduction of current to Blumleins pulse forming lines commenced either through top copper electrode holders or base copper electrodes depending on integrity of switch contacts to these electrodes in some locations. Discontinuities on the surface of the switch and the top copper electrodes holders prohibited power coupling with the Blumlein power source through these electrodes in some locations, thereby directing the current conduction through the back of the switch and base electrodes. This caused more damage to the back of the switch at some contact points. Inversely, due to the poor contact between the base electrodes and the switch in other locations, current conducted through the front of switch and top copper electrodes, causing more damage to the front of switch.

We continued the experiments by using a GaAs switch with no coating. Similar results for the switch lifetime were obtained. The switch commutated the pulser at 72 MW for about 3 x 10^3 shots after which it was failed. Again, the switch damage appeared on both sides of the switch as shown schematically in Fig. 27. Comparison of output pulses generated by commutating the pulser with these two types of switch, however, showed a better pulse integrity for the switch with the Ge contact. Waveform rising edges had smaller step-like shape and so

the pulse risetimes were slightly faster. It seemed that the flow of charge between electrode and switch was better in this case.

Switch longevity was further studied by using GaAs switches with multi-layer metal contacts. Two types of switch were used. The first type was obtained from U.S. Army research laboratory. It had metal contacts consisted of 15 nm Ni/ 75 nm Ge/ 75 nm Au/ 75 nm Pd/ 200 nm Au. The second type was fabricated in house by depositing metal contacts consisted of 125 nm Ge followed by 250 nm mixture of Au and Pd. These switches were tested under similar conditions of experiment as described earlier. The switch lifetimes were 2×10^3 and 3×10^3 commutation cycles for the first and the second switch, respectively. Figure 28 represents a photograph of the first switch after 1500 shots. The electrode positions are plotted in this figure for reference.

Examination of damage on this switch indicated the conduction of current both laterally and also through the thickness of the contact. It seemed that for the initial cycles of commutation, current was conducted in narrow channels laterally until high current density evaporated Au and Pd which subsequently condensed on the switch gap as seen in Fig. 28. Afterward, the current conducted through the contact thickness and into GaAs as it did in our earlier experiments. Lifetime study for the second switch fabricated in our laboratory showed similar damage mechanisms but longer lifetime. Output pulses generated were found similar for both switches. Examination of the switches in these experiments as shown in Figs. 27 and 28 showed more damage and erosion near the cathode. This suggested the initiation of avalanche processes near the cathode areas. It appeared that for the conditions of our experiments, switch lifetime did not improve by deposition of multi-layer metal contacts. This was due to current conduction with very high densities in a narrow channel, causing damage to the switch.

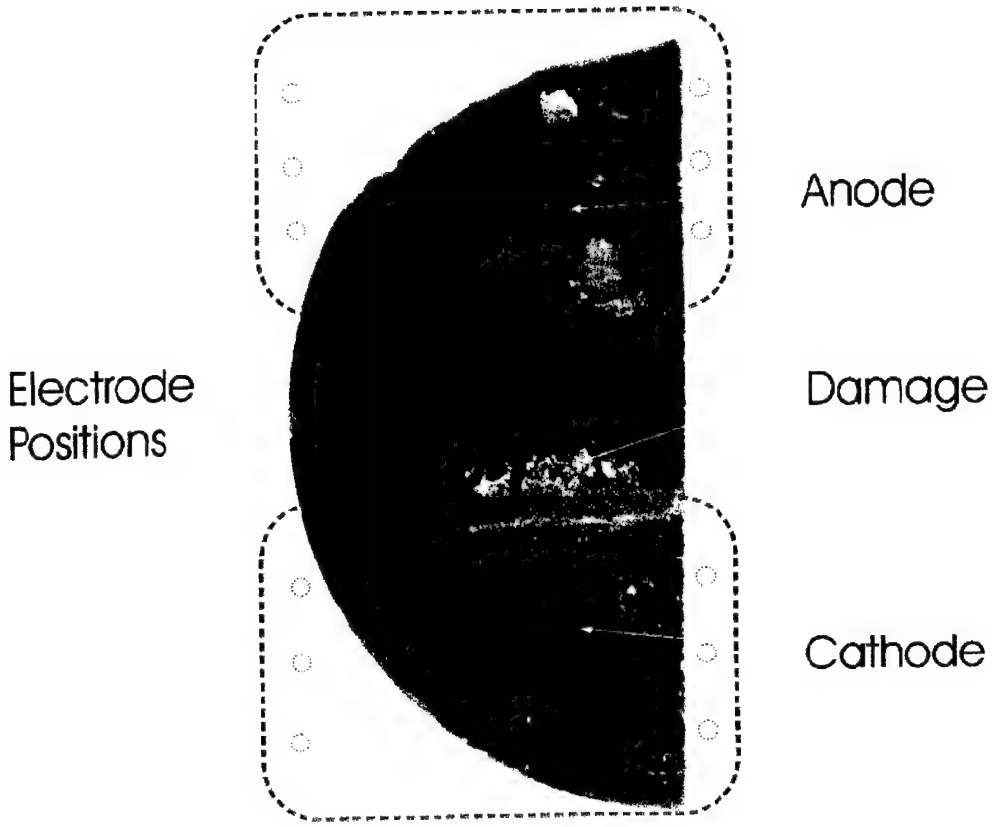

Figure 28. Photograph showing appearance of damage on a GaAs switch with multi-layer contact used to commutate the stacked Blumlein pulser at 72 MW for 1500 shots. The electrode positions are plotted in this figure for reference.

5. Switch Lifetime Studies Using Amorphic Diamond

For the sake of consistency, we placed layers of Kapton insulator between the switch and the base electrode to restrict the current path through the top electrodes and so only switch front contacting the top electrode holders was affected and damaged. In this configuration, we performed the switch longevity experiment with a bare GaAs switch with no metal contacts.

For these studies the modified CPC was used to charge the 2-line B pulser (version 2) in about 20 ns. The switch commutated the pulser at 72 MW (1.2 kA current) for 5×10^3 shots after which it failed and switching was stopped. A negative photograph of this switch after completing the test is shown in Fig. 29(a) for reference. The switch gap is presented by the two horizontal lines of damage at the limit of the copper plate electrodes not shown in the figure. The damage line shown at the bottom of Fig. 29(a) corresponds to the cathode side. More damage is seen at the cathode electrode contact. It appears that the damage at the electrode contact areas eventually caused thermal runaway at the switch gap surface and produced a crack that shorted the gap. Figure 29(a) clearly shows two branches of damage propagating from cathode to anode in the switch gap.

We continued the lifetime studies with a GaAs switch coated with a 1-cm strip of amorphic diamond at the cathode location. The film thickness was 600 nm. The switch assembly permitted a switch gap of 12 mm with diamond strip extended about 5 mm into the gap. The switch was tested under similar conditions of experiment as described earlier for the uncoated PCSS. The switch lifetime was found to be 1×10^4 commutation cycles after which switching was stopped.

Examination of switch revealed branches of damage extending from the cathode to anode electrode contact locations in the switch gap. For comparison, Fig. 29 (b) presents a negative photograph of the switch after 5 x 10^3 shots. The switch damage is located at the limit of the copper plate electrodes not shown. The damage line shown at the bottom of Fig. 29(b) corresponded to the cathode side and showed less damage as compared to the anode damage line shown at the top of this figure. No appreciable damage was observed at the switch gap between the two electrode contact areas seen by the two horizontal damage lines in Fig. 29(b). With the application of amorphic diamond, not only the switch lifetime was increased but also the damage at the cathode contact was found to be less than that found for the anode contact. This indicated that the diamond coating protected and hardened the cathode side.

Figure 30 presents schematic diagrams of the current filamentation examined during these experiments with the aid of an infrared viewer. The left plot of this figure shows the LD-220 laser beam focused in two lines on the switch. In experiments where the switch had no diamond coating, the majority of the time, a single current filament commutated the switch. The filament was initiated near the cathode and followed, approximately one of the laser beams to the anode. Multiple branching of the filament was rarely seen. In the case of switch with the diamond coating, the multiple branching was observed more often indicating an increase of pre-avalanche sites.

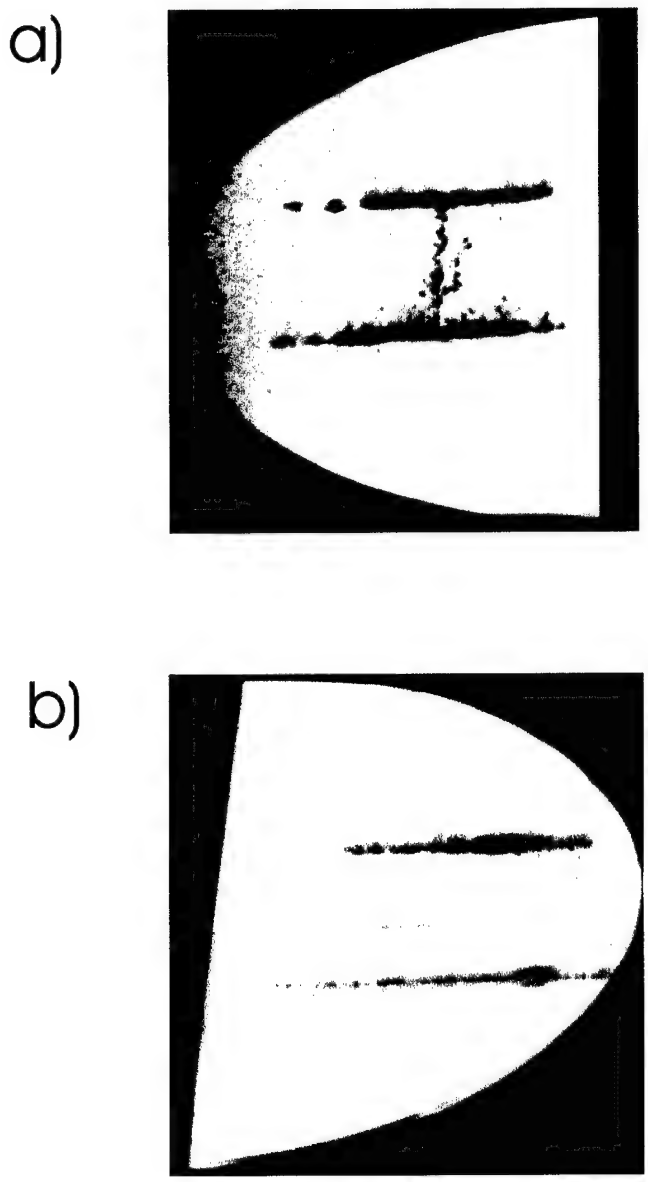

Figure 29. Photographs showing (a) a GaAs switch with no contact (b) a GaAs switch with the amorphic diamond coating, after 5 x 10^3 cycle of commutation at 72 MW.

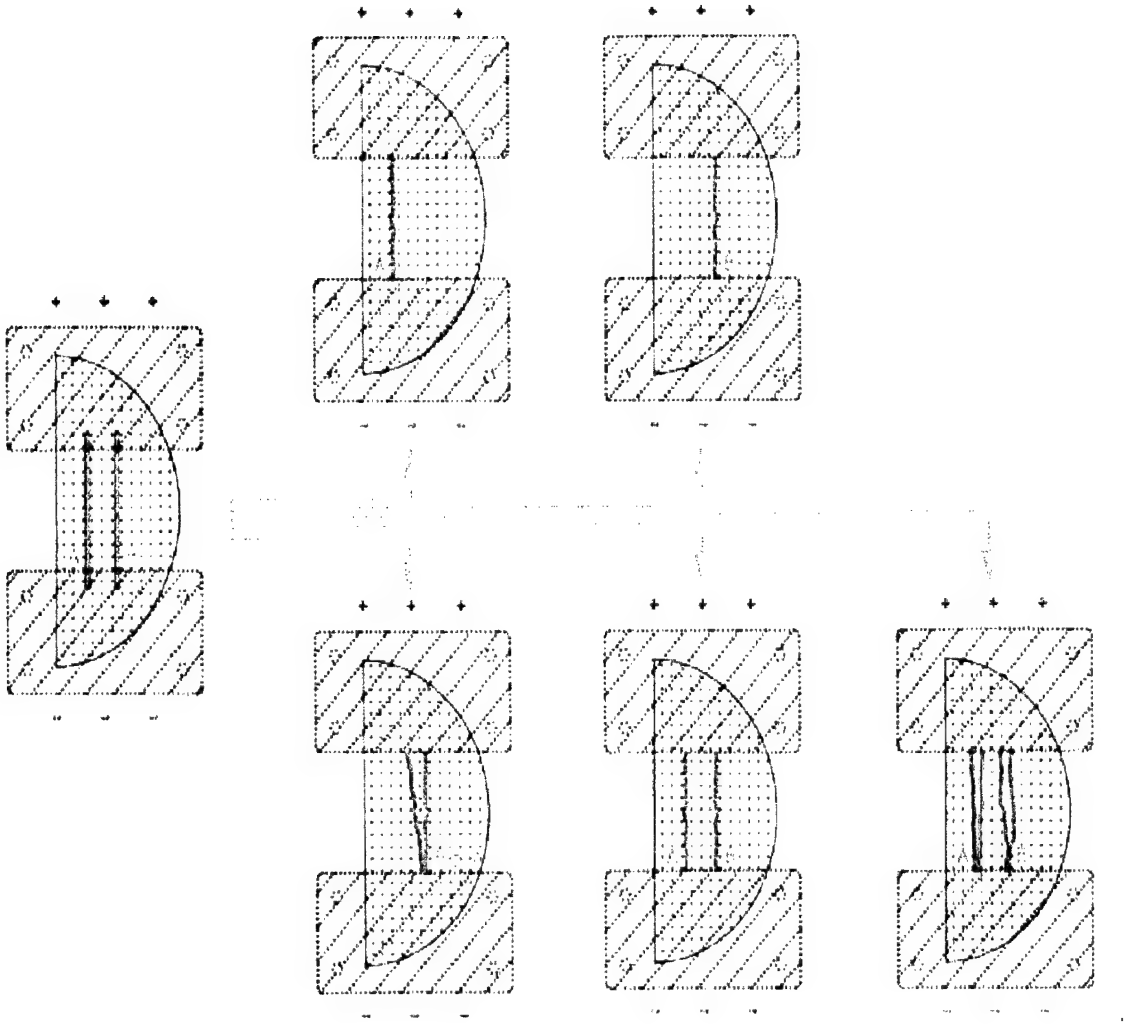

Figure 30. Schematic diagrams of the LD-220 laser diode beam focused on the switch, and current filamentation seen with an infrared viewer during this work.

AMORPHIC DIAMOND COATINGS

1. General Properties

Basic research in our laboratory has already described a conformal coating that has hardness of natural diamond and exceptionally high values of electron emissivity. Discovered at UTD, it is made from graphite and laser light without catalyst, or toxic wastes. It was termed amorphous ceramic diamond and later shortened to "amorphic diamond" for convenience. Deposited at room temperatures it forms a strong bond to any material onto which it is applied. Such a favorable combination of hardness, chemical bonding and an elastic modulus of 850 GPa should translate directly into an increased resistance to abrasive wear of components coated with amorphic diamond. It has been demonstrated that only a 1-3 μm coating of amorphic diamond could protect fragile substrates against erosive environments.

The experimental conditions used at UTD to deposit films of amorphic diamond have been described previously [14-21]. A Q-switched Nd-YAG laser was used to deliver 250 - 1400 mJ to a graphite feedstock in a UHV system at a repetition rate of 10 Hz. The beam was focused to a diameter chosen to keep the intensity on the target near 5×10^{11} W cm^{-2} and the graphite was moved so that each ablation occurred from a new surface. A high current discharge confined to the path of the laser-ignited plasma was used to heat and process the ion flux further

Amorphic diamond is distinguished by the combination of its unique microstructure shown in Fig. 31 together with the mechanical properties of diamond it displays. Analytical techniques have shown it to consist of nodules of tens of nanometers in diameters that are composed of sp3 (diamond) bonded carbon in a matrix of other carbons. The diamond character has been attested by the agreement of structural morphology, density, optical properties, Ka line energies and hardness.

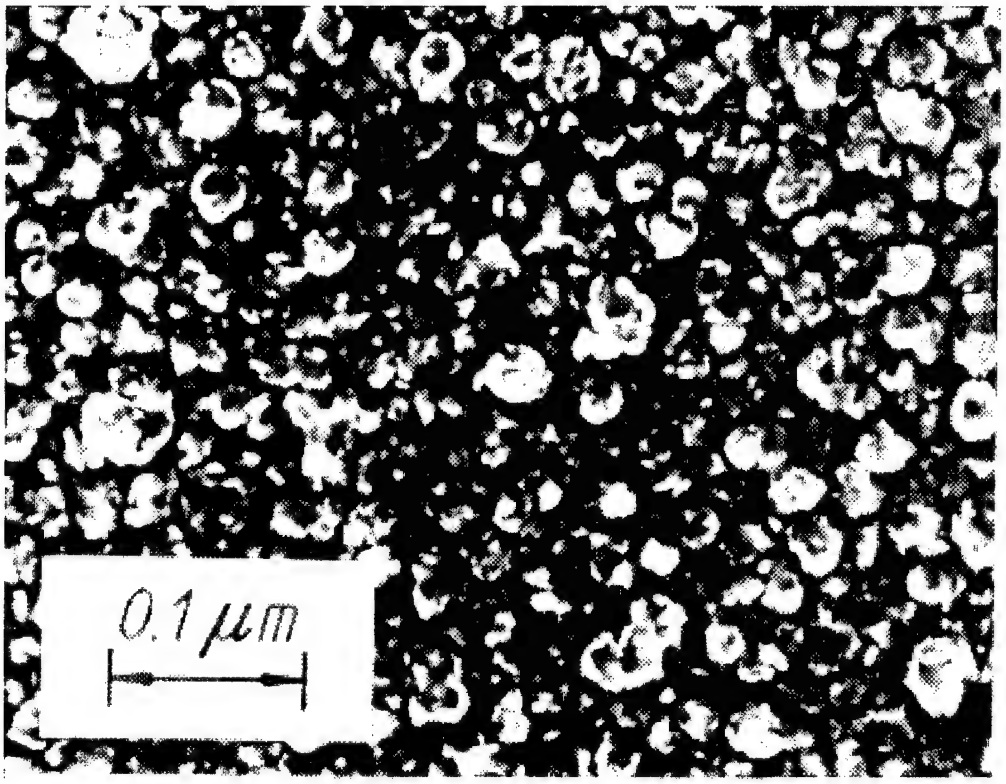

Figure 31. Diamond nodules shown by transmission electron microscopy (TEM) of a gold coated replica of a film of amorphic diamond.

Nuclear reaction analysis (NRA) has proven the hydrogen content to be less than 0.5%. The nodules seem to be disordered mixtures of the cubic and the rare hexagonal polytypes of diamond that have no extensive crystalline planes along which to fracture. Such disorder creates strains that are balanced by the large surface energies available at nanometric scales. The ceramic that results from packing the nodules is surprisingly free from internal stress. Values of compressive stress measured in finished films of micron thickness are low for amorphous materials, being 0.5 to 0.8 GPa. Since it is condensed from laser plasmas produced under conditions, which are also optimal for the growth of interfacial layers, the films of amorphic diamond are strongly bonded to the substrates onto which they are condensed [14-21].

2. Semiconductor Properties of Amorphic Diamond

1. Field emission

Because of the potential for use in cold cathode devices, flat-panel displays and photoconductive switch development, the emissivity of electrons from amorphic diamond layers is of considerable interest. The original speculation was that the use of natural diamond as a field emitting material would encounter problems of recharging after emission because of the high resistivity of diamond. However, nodules of diamond in a matrix of more conductive phases of carbon might provide better field emission. Measurements of electron emissivity confirmed this expectation in studies comparing the performance of planar films of amorphic diamond that contained nodules of diamond with layers of defected graphite that had pointed structures of similar size to nodules. Films were prepared on similar Si substrates, but amorphic diamond were condensed from C^{3+} and C^{4+} plasmas at high laser intensities while the defected graphite was condensed from material passing the periphery of the ablation plume [16].

Measurements of electron emissivity are conveniently described in terms of the Fowler-Nordheim model, which parameterizes the emitted current density, J (A cm^{-2}) as a function of the electric field strength, E (V cm^{-1}) in which the sample is immersed,

$$J = (1.54 \times 10^{-6})\, ß^2 E^2 \Phi^{-1} \exp\left[-(6.83 \times 10^{7})\, \Phi^{1.5} ß^{-1} E^{-1}\right] \qquad (1)$$

where ß is the enhancement of local electric field; S is the effective emitting area; I is the current and Φ is the work function. As can be seen, a graph of the logarithm of I/E^2 as a function of 1/E should be linear. Data of the type needed for comparison with the Fowler-Nordheim model was obtained with the apparatus shown schematically in Fig. 32. In a vacuum environment, an anode probe with a 0.5 mm radius of curvature was moved with micrometric precision toward a cathode consisting of a silicon wafer coated with the emissive material to be characterized. The field strength was computed from the applied voltage and the anode to cathode separation and the current was measured directly. Results for conventional Spindt microtips fabricated on silicon surfaces [22], defected graphite and amorphic diamond coatings are shown in Fig. 33.

The most striking aspect of the data of Fig. 33 is the extent to which all of the noncrystalline carbons emit a given current density at nearly an order of magnitude lower voltage that needed for a cathode of microtips. On a finer scale of inspection it can be seen that for a given voltage a cathode of amorphic diamond emits an order of magnitude more current density than does a cathode of defected graphite. In Fig. 33 the data for "nominal" amorphic diamond is characteristic of the type of film that is usually used in mechanical studies of wear and tribology. It consists of about 75% (by volume) of diamond nodules as seen, with the balance being more conductive phases in which the nodules are embedded. However, the fraction and packing of nodules can be adjusted during deposition, and emissivity data for two options are included in Fig. 33.

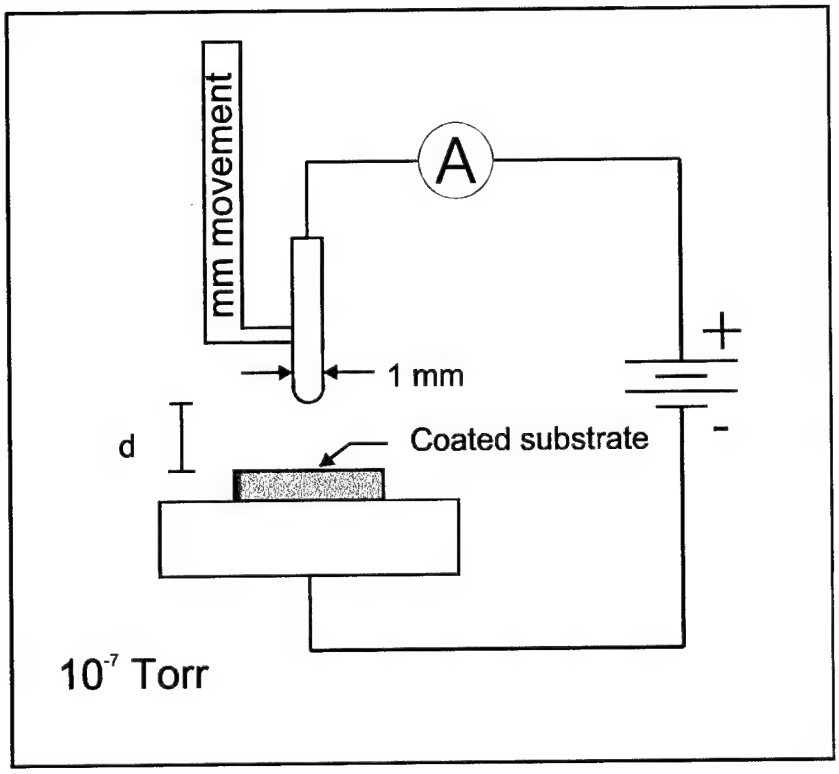

Figure 32. Schematic representation of the apparatus used in characterizing the high field emissivity of electrons from types of diamond films.

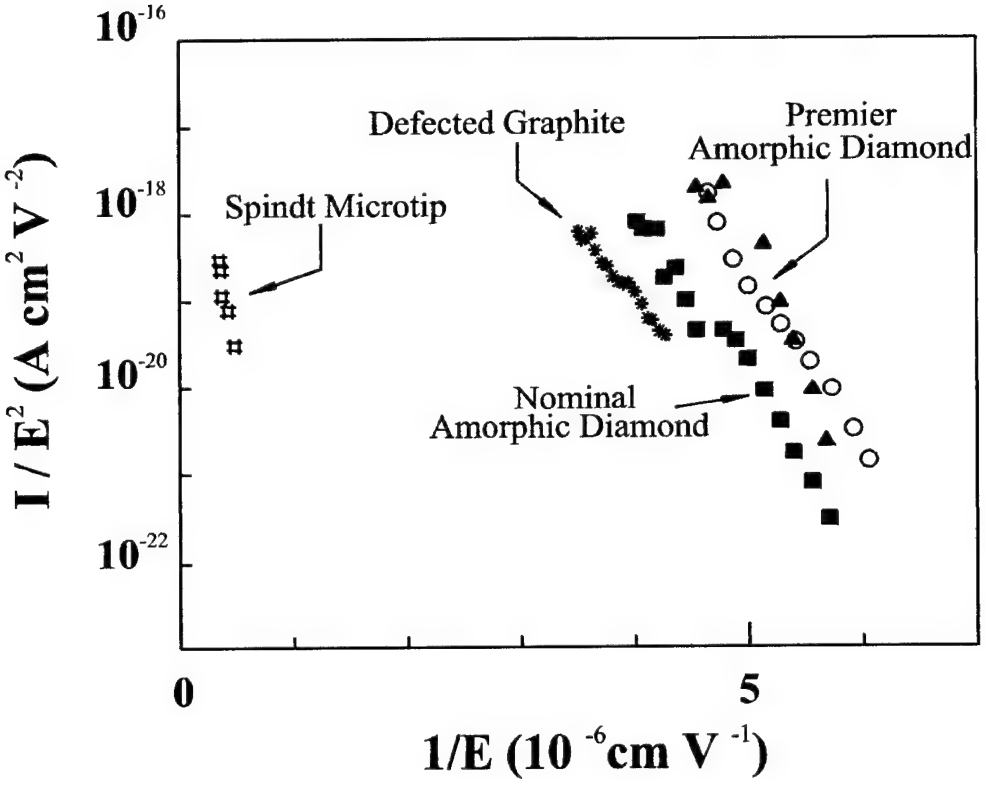

Figure 33. Plots of emission current, I per unit field strength squared, E^2 as functions of the inverse electric field strength, 1/E from cathodes coated with various diamond materials to facilitate comparison with the Fowler-Nordheim model.

2. Formation of rectifying heterojunctions

In this research, amorphic diamond coatings were deposited on one side of Si substrates and electrodes were attached to either side using conducting silver paint and epoxy. The grid-like conducting electrodes were painted on the coating sides. For these measurements a Keithley 237 high voltage source-measure unit was used to provide constant voltage bias while monitoring the current through the sample. To avoid heating the sample the measurements were carried out with pulsed voltage sweep having on and off times of 50 and 450 ms, respectively. For measurements of forward diode characteristics, diamond coating was biased negative with respect to the substrate. Under white light conditions, the total luminous flux received on a unit area (illuminance) of the sample was measured by a light meter. Typical I-V characteristics measured for a 0.22 μm premier amorphic diamond on the p-type Si (100) with a resistivity in the range 20-60 Ωcm are shown in Fig. 34. To qualify as "premier" the film was deposited at higher laser intensities [16] and had a mass density and an optical gap of 2.6 g cm^{-3} and 1.6 eV, respectively.

The rectifying behavior seen in Fig. 34 was attributed to the amorphic diamond /Si junction. This was verified by placing silver epoxy electrodes on bare Si substrates and observing a symmetrical and ohmic current-voltage behavior with change in voltage polarity. Figure 35 plots data for current versus illuminance under reverse biased conditions and white light. Current increases of one to two orders of magnitude were observed when the device was exposed to light. Under forward biased conditions there were only slight current increases for the light exposure. For all devices fabricated the maximum of the photoresponse was found to be in the range 600 – 900 nm.

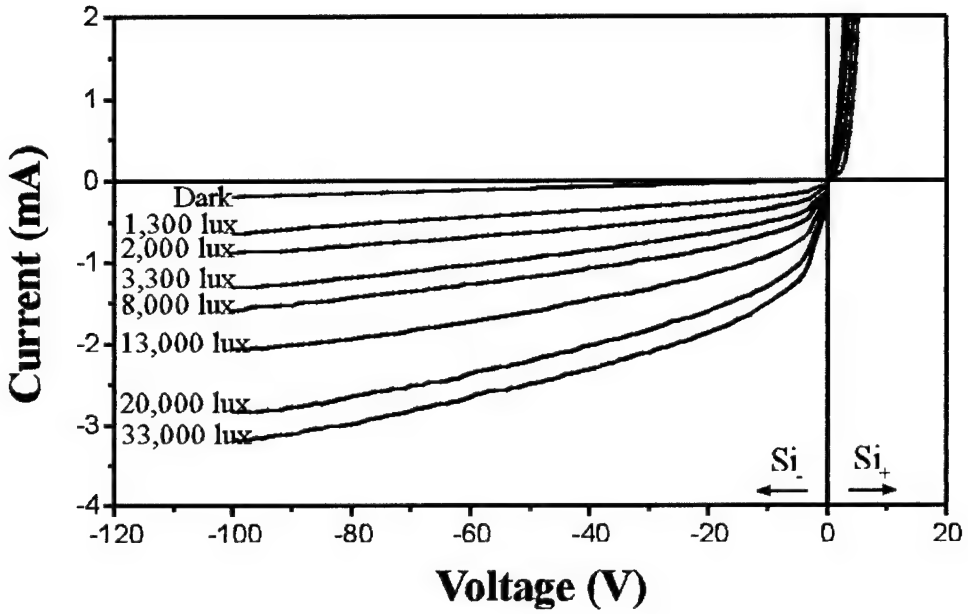

Figure 34. Current-Voltage characteristics measured for an amorphic diamond film deposited on a p-type Si in the dark and under white light conditions.

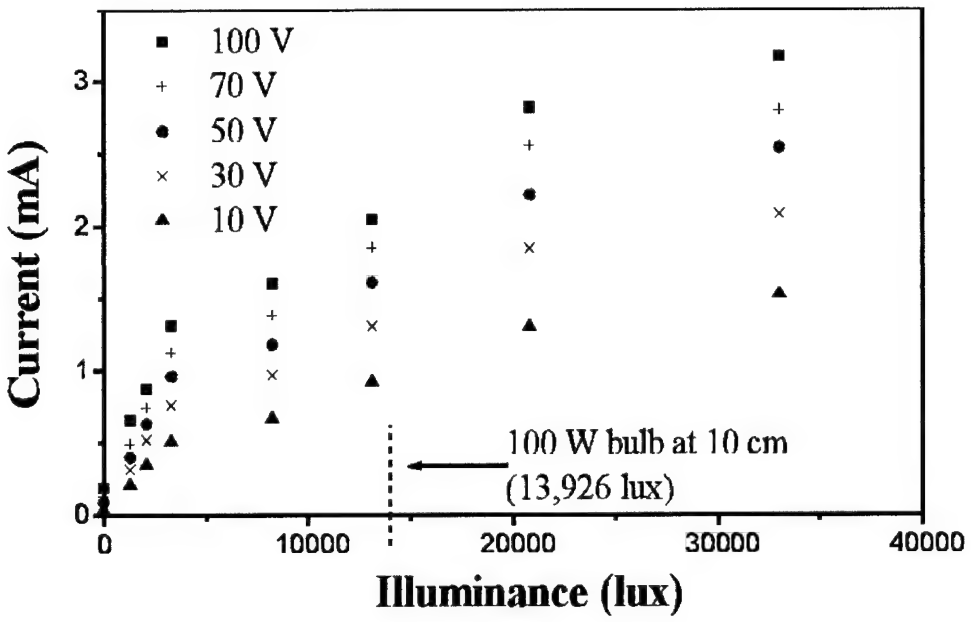

Figure 35. Current conducted at different reverse bias voltages for an amorphic diamond / p-type Si device under white light condition.

We also examined in the dark, the I-V characteristics of 0.3 μm nominal amorphic diamond films on three p-type Si (100) samples with different conductivities. Results are shown in Fig. 36. The terms: high, medium and low correspond to Si substrates with resistivities in the range of > 2000 Ωcm, 20-60 Ωcm and 0.01-0.02 Ωcm, respectively. For the sample with the low resistivity Si, the I-V characteristics was more symmetrical and ohmic with a forward and reverse bias dynamic resistance values of about 47 and 65 Ω, respectively. For the devices with the medium and high resistivity Si, however, highly asymmetric I-V plots were obtained which indicated formation of rectifying heterojunctions. It should be noted that while the forward dynamic resistance values for all the devices were about the same, the reverse dynamic resistance values were considerably different. For the samples denoted medium and high the values were about 23 kΩ and 70 MΩ, respectively. Figure 37 compares the I-V characteristics obtained in the dark for the coated sample denoted high and an uncoated similar Si substrate. A symmetrical and ohmic behavior is seen for the uncoated sample. Of importance is the rapid current increase in forward direction for the coated sample. This is attributed to the tunneling of electrons from amorphic diamond to the conduction band of the Si, a process similar to the Fowler-Nordheim tunneling. Similar studies were also performed for the samples denoted medium and low and results showed much less tunneling effects as expected.

Current-voltage properties were also studied for the amorphic diamond on n-type silicon. It was found that rectification was in the same direction with diamond layer acting as the cathode. Figure 38 compares the I-V characteristics, in the reverse biased conditions, for the nominal amorphic diamond coatings 0.23 and 0.13 μm-thick on the n-type and p-type Si substrates, respectively.

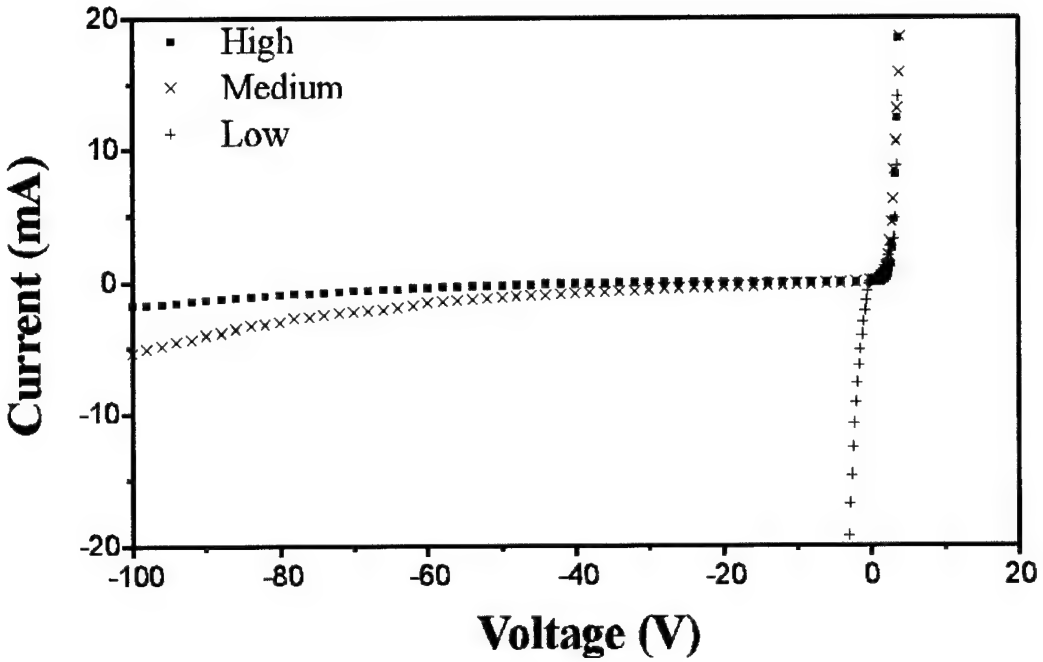

Figure 36. Current-Voltage characteristics measured in the dark for nominal amorphic diamond films deposited on p-type Si substrates with a resistivity ratings of high, medium and low.

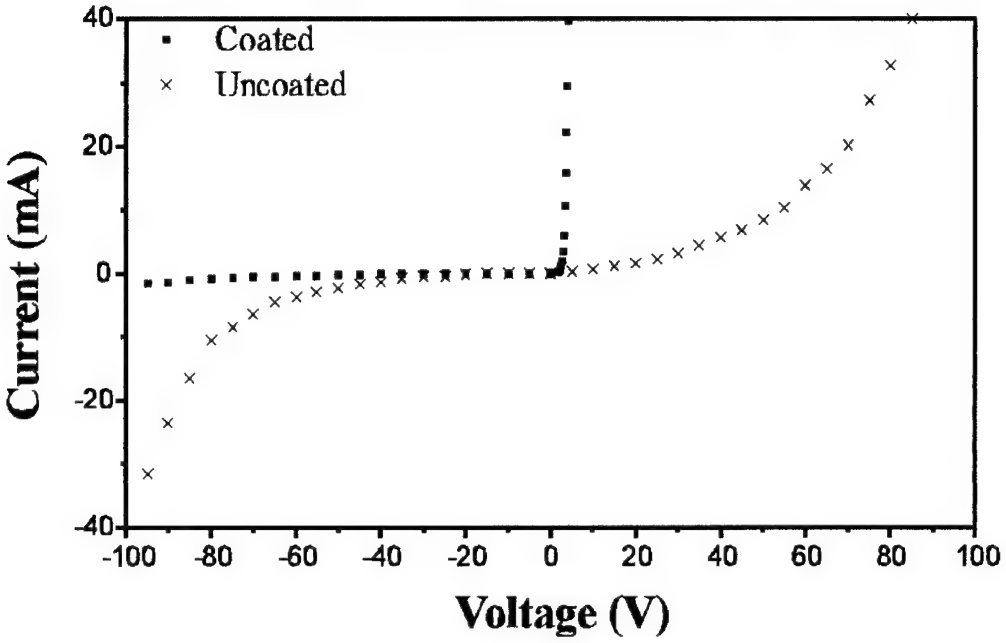

Figure 37. Current-Voltage characteristics measured in the dark for an uncoated and diamond coated Si with a high resistivity rating.

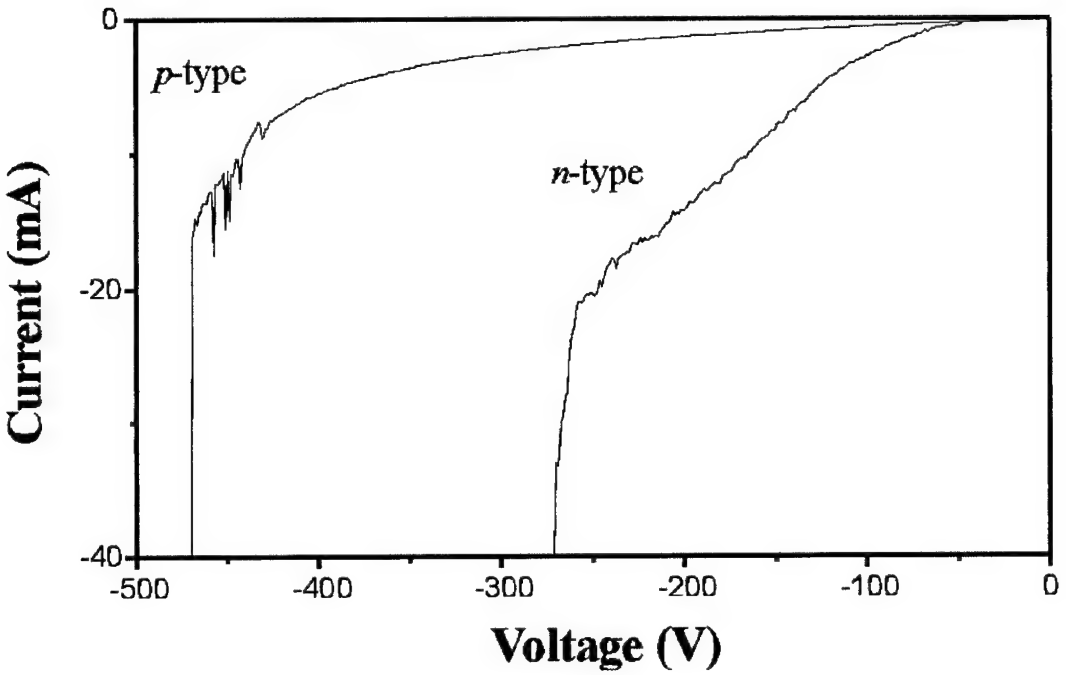

Figure 38. Current-Voltage characteristics showing the breakdown voltages for the nominal amorphic diamond films on p- and n-type Si substrates. Measurements were performed in the dark under reverse bias conditions.

The measured reverse breakdown voltage in excess of 425 V for a 0.13 μm-thick coating on p-type Si gives an electrical breakdown strength greater than 3 x 10^9 V/m if the entire diamond film is assumed to be depleted. The high electrical breakdown strength for amorphic diamond suggests that carrier velocity saturation in high field strength is allowed and the electron-electron scattering is of the same order as that in crystalline diamond [23]. In almost all junctions fabricated, the reverse breakdown voltage of the amorphic diamond on n-type Si appeared to be less than that on p-type Si. As shown in Fig. 38, a thicker film of amorphic diamond on n-type Si had a lower reverse breakdown voltage and the breakdown strength was about 1.1 x 10^9 V/m. In addition, for the sample comprised of n-type Si, a soft breakdown of reverse voltage is seen at around 60 V. This may be due to the release of trapped negative charges when the amorphic diamond is slowly depleted at reverse bias voltages above 60 V.

We performed experiments to test these amorphic diamond / silicon rectifying devices as low voltage photoconductive switches. For this purpose, a single Blumlein with line length of 3.6 m and Blumlein impedance of 50 Ω was constructed. Output of the Blumlein was connected to a 50 Ω, non-inductive carbon disc resistor. Switching and storage capacitance of the Blumlein was about 1 nF. An amorphic diamond /silicon device was connected to the Blumlein in a reversed biased configuration where the anode electrode was attached to amorphic diamond side. A pulse charging power supply was used to charge the Blumlein in about 50 μsec, after which a trigger pulse from a master oscillator Q-switched an Nd:YAG laser and provided trigger photons in a 40-ns FWHM pulse for the switch activation. Output voltage waveform is shown in Fig. 39 for the charging voltage of 100 V. It is interesting to note that these rectifying devices acted as linear photoconductive switches where switch voltage follows closely the activating laser pulse.

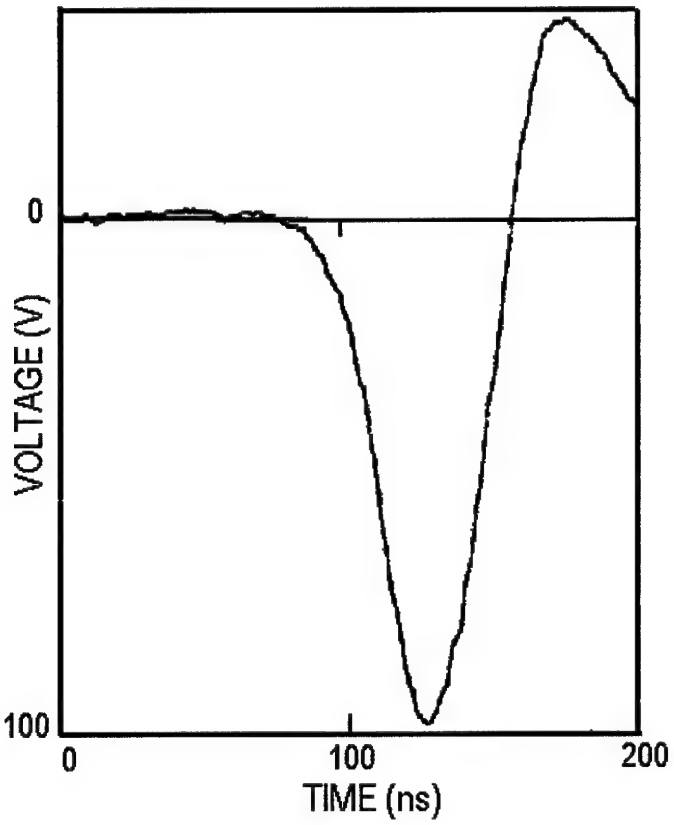

Figure 39. Voltage waveform generated by a single Blumlein pulser using a diamond/Si heterojunction device as the photoconductive switch. Charging voltage was 100 V.

In these studies, we also examined the I-V characteristics of amorphic diamond on a semi-insulating GaAs with resistivity of about 1.0×10^7 Ωcm, the type used in our stacked Blumleins as the photoconductive switch material. Results are presented in Fig. 40 for a bare GaAs sample and a 0.57 μm amorphic diamond film on GaAs in the dark. A symmetrical and ohmic current-voltage behavior is seen for the uncoated substrate. The I-V characteristics differ considerably for the diamond-coated sample measured in the dark, especially for the forward current region where the coating side was biased low. This may be due to the release of trapped negative charges when the amorphic diamond is slowly depleted at reverse bias voltages above 300 V. Of importance to this study, is the rapid current increase in forward direction. This is attributed to the tunneling of electrons from amorphic diamond to the conduction band of the GaAs. This process is similar to the Fowler-Nordheim tunneling. It may provide pre-avalanche sites for operation of diamond coated PCSS and diffuse the conduction current.

Further studies are needed to obtain the precise mechanism of heterojunction operation and to clearly identify the device category and relation to the other diamond based heterojunction devices [24-29]. However, it appears that the amorphic diamond conducts by a tunneling process or thermally assisted hopping at or near the Fermi level while the Si or GaAs conducts by an emission process. The free charge density of amorphic diamond being higher than that of the crystalline semiconductor causes the heterojunction to exhibit a Schottky like barrier properties to the extent that the reverse bias characteristics are voltage dependent. The effect of image force lowering of the Schottky barrier is very slight and the conduction through the device is accomplished by the majority carriers through the recombination at the interface. Existence of a high density of interface states is evidenced by the direction of rectification being independent of crystalline substrate impurity types.

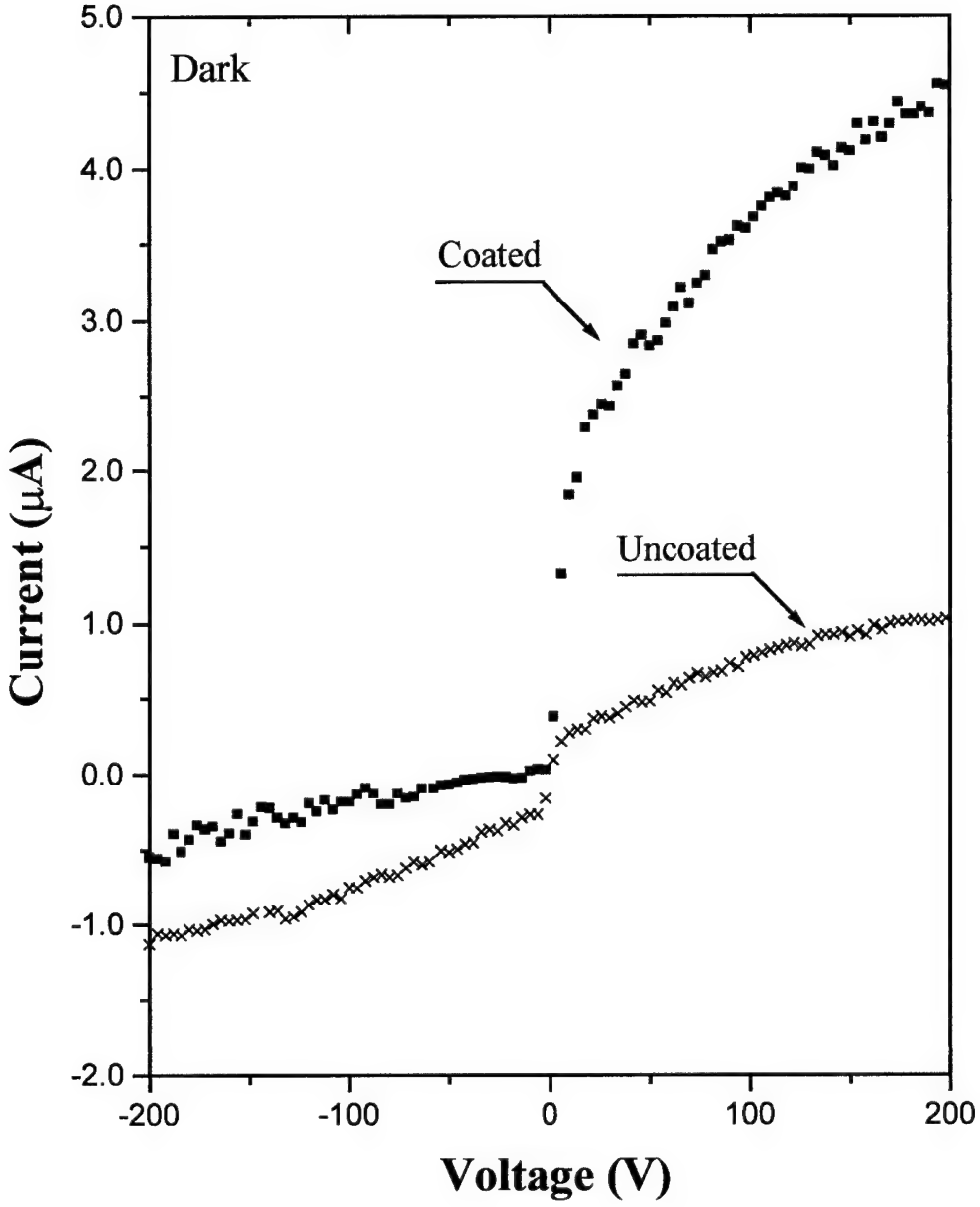

Figure 40. Current-Voltage characteristics measured for an uncoated and diamond coated GaAs in the dark.

CONCLUSIONS

Advances in stacked Blumlein technology for voltage multiplication at UTD, including progress made during this research program, offer exciting possibilities for a variety of ultra-wideband (UWB) applications especially in array UWB and compact UWB sources. Some of these sources are being used for synthetic aperture radar applications that inherently use the frequency content of pulses. At the 100 MW level of power, broad-band sources operating at kiloHertz repetition rates can be conceived that simply match compact pulsed power devices to the radiation impedance of free space.

The rapidly growing field of HPM technology currently progresses in two directions of narrowband radio frequency (RF) sources and ultra-wideband (UWB) emitters and antennas. Sources employing UWB schemes feature fast rising, short pulse width waveforms and have a broad frequency content. Basically, the development of UWB sources are also being pursued in two directions. The first uses a single pulser to feed a very high voltage to a single antenna. The second employs many radiating elements each powered with a separate pulser synchronized together to produce an additive field at the target (array UWB source). The stacked Blumlein technology offers significant advantage for the array source concept by delivering higher voltage to each radiating element than that available with existing photoconductively -switched systems.

Conventional attempts to utilize photoconductive switches have focused upon nonlinear commutation of pulsers with PCSS devices. However, a persistent problem in switch lifetime has limited the wide use of the switch in high power applications. Filamentation of the conductivity associated with the high gain GaAs switches produces such high current density that the switches are damaged near the metal – semiconductor interface and the lifetime is severely limited.

During this research program, a substantial effort was directed to study and implement the broadening of the current channels in the avalanche photoconductive switch in order to improve lifetime and increase switching peak power. This was performed by the control of laser diode beam delivery to the switch, improvement of switch contacts, pulser configuration and charging mechanism. We also studied the use of amorphic diamond film as photoconductive switch coating to improve the longevity and operation of PCSS devices in stacked Blumlein pulsers. Experiments were conducted with a PCSS fabricated by the deposition of amorphic diamond film near the switch cathode contact. A significant improvement in switch lifetime was resulted by testing the performance in a prototype pulser. It appeared that not only the diamond coating protected and hardened the cathode side but it also helped branching the filaments conducting high currents.

Semiconductor properties of amorphic diamond relevant to PCSS application were examined by the fabrication and testing of heterojunction devices formed between amorphic diamond and crystalline semiconductors and by studying field emission characteristics. The results indicated formation of rectifying heterojunctions between amorphic diamond and PCSS switch material exhibiting highly asymmetric I-V characteristics. It was found that current was rectified in the same direction with the diamond layer biased negative acting as the cathode. In addition, it was demonstrated that amorphic diamond emitted electrons at high current densities when immersed in modest electric field strengths and the electron emission could be adjusted by modifying the process parameters for the film production.

Encouraging or inhibiting the field emission characteristics and the current conduction flow at the interface between amorphic diamond and PCSS material may have prominent effect upon off-state switch hold-off and switch performance. The switch lifetime studies performed in

this work seemed to indicate an increase in pre-avalanche sites due to the semiconductor characteristics of amorphic diamond discussed. Further studies, however, are required to obtain precise conduction mechanism of the PCSS coated with amorphic diamond.

In addition to our own effort using amorphic diamond, there are intensive research programs in direction of improving PCSS lifetime in pulsed power systems. The longevity of the PCSS at low power applications has been improved by doping the semi-insulating GaAs underneath the metal contacts [30]. Other efforts have focused on an opposed-contact PCSS with an n^+ region next to the cathode electrode. Increased hold-off characteristic of this class of devices has been analyzed by simulation and it is shown that the introduction of the n^+ region inhibits the flow of electrons at the interface until very high fields are reached [31]. Photoconductive switch enhancements realized in this work are well complementary and strengthen these efforts by utilizing unique semiconductor properties of amorphic diamond. Further research is underway to study and characterize the elementary processes involved in conduction of PCSS devices coated with amorphic diamond.

EXECUTIVE SUMMARY

1. Summary of the Results

The objective of the research conducted under this grant was to enlarge the stacked Blumlein technology base, level of understanding, and the pulser design options that make optimal use of the promising capabilities of the photoconductive semiconductor switches (PCSS) in an Ultra-Wideband (UWB) source. During this research, Several photoconductively-switched stacked Blumlein prototype pulsers were tested under different conditions of operation at power levels approaching 100 MW. Special attention was placed on broadening of the current channels in the avalanche photoconductive switch in order to improve PCSS lifetime. Switch longevity was tested by fabricating switch with metal or diamond coatings and by implementing different switch/electrode configurations. A significant improvement in switch lifetime was resulted by testing the diamond-coated switch performance in a prototype pulser. The following Table presents the best simultaneous and individual results obtained, to date, by switching the stacked Blumlein pulsers with a high gain GaAs photoconductive semiconductor switch (PCSS).

Parameters	Simultaneous Results	Individual Results
Switch Voltage	60 kV	100 kV
Switch Current	1.2 kA	2 kA
Pulse Risetime	200 ps	150 ps
R-M-S Jitter	500 ps	200 ps
Optical Trigger Energy	300 nJ	300 nJ
Repetition Rate	10 Hz	200 Hz
Electric Field	60 kV/cm	100 kV/cm
Stack Voltage	112 kV	175 kV
Switch Lifetime	1×10^4 pulse	1×10^5 pulse

In order to obtain an understanding of electrical conduction mechanisms, a substantial effort was directed to examine semiconductor properties of amorphic diamond coatings on conventional crystalline semiconductors. Deposition of thin films of amorphic diamond on both Si and GaAs crystalline substrates produced rectifying heterojunctions with highly asymmetric I-V characteristics. Regardless of the doping type and its concentration, the current was rectified in the same direction with diamond layer acting as the cathode. When reversed biased, current levels from the heterojunction varied with the amount of reverse bias and the illumination and a photoconductive effect was observed. Measurements indicated an electrical breakdown strength

of better than 3 x 10^9 V/m for the amorphic diamond. The diamond/Si heterojunction devices were tested as photoconductive switches in our Blumlein pulsers where they successfully commutated the pulsers at low powers.

In addition, it was demonstrated that amorphic diamond emitted electrons at high current densities when immersed in modest electric field strengths and the electron emission could be adjusted by modifying the process parameters for the film production. Encouraging or inhibiting the field emission characteristics and the current conduction flow at the interface between amorphic diamond and PCSS material may have prominent effect upon off-state photoconductive switch hold-off and performance. The switch lifetime studies performed in this work seemed to indicate an increase in pre-avalanche sites due to the semiconductor characteristics of amorphic diamond discussed.

2. Personnel Participated

The professional personnel participated in the research program are listed below:

1) Carl B. Collins	Professor
2) Farzin Davanloo	Research Scientist
3) Hwantae Park	Postdoctoral Research Associate
4) Remi Dussart	Graduate Student
5) Mugurel C. Iosif	Graduate Student
6) K. Jarmo Koivusaari	Graduate Student

3. Publications

F. Davanloo, H. Park, R. Dussart, M.C. Iosif, C.B. Collins and F.J. Agee, "Progress in the Development of Stacked Blumlein Pulsers Commutated by Photoconductive Switches," in Conference Record of the 1998 Twenty-Third International Power Modulator Symposium, Rancho Mirage, CA, June 22-25, 1998, pp. 144-148.

F. Davanloo, C. B. Collins and F. J. Agee, "High-Power, Repetitive-Stacked Blumlein Pulsers Commutated by a Single Switching Element," IEEE Trans. Plasma Sciences, 26, 1463 (1998).

F. Davanloo, H. Park, C. B. Collins and F. J. Agee, "Photoconductive Switch Enhancements for Use in Stacked Blumlein Pulsers," in Proceedings of the 15th International Conference on Application of Accelerators in Research and Industry, Denton, TX, Nov. 4-7, 1998 (AIP Conference Proceedings 475, 1999, Woodbury, New York), pp 918-921.

F. Davanloo, R. Dussart, M. C. Iosif, C. B. Collins and F. J. Agee, "Photoconductive Switch Enhancements and Lifetime Studies for Use in Stacked Blumlein Pulsers," in Proceedings of the 12th IEEE International Pulsed Power Conference, Monterey, CA, June 27-30, 1999, pp. 320-323.

F. Davanloo, R. Dussart, K. J. Koivusaari, C. B. Collins and F. J. Agee, "Photoconductive Switch Enhancements and Lifetime Studies for Use in Stacked Blumlein Pulsers," accepted for publication in IEEE Trans. Plasma Sciences, Oct. 2000.

F. Davanloo, C. B. Collins, K.J. Koivusaari, and S. Leppävuori, "Amorphic Diamond / Silicon Semiconductor Heterojunctions Exhibiting Photoconductive Characteristics," accepted for publication in Appl. Phys Lett., Sept. 2000.

REFERENCES

[1] A. D. Blumlein, U.S. Patent No. 2 465 840, 1949.

[2] C. B. Collins, F. Davanloo and T. S. Bowen, Rev. Sci. Instrum. 57, 863 (1986).

[3] F. Davanloo, T. S. Bowen and C. B. Collins, Rev. Sci. Instrum. 58, 2103 (1987).

[4] T. S. Bowen, Ph.D. Dissertation, University of Texas at Dallas, 1988, Unpublished.

[5] F. Davanloo, J. J. Coogan, T. S. Bowen, R. K. Krause, and C. B. Collins, Rev. Sci. Instrum. 59, 2260 (1988).

[6] J. J. Coogan, F. Davanloo, and C. B. Collins, Rev. Sci. Instrum. 61, 1448 (1990).

[7] C. B. Collins, F. Davanloo, "Feasibility of a GW Pulser to Supply HPM Systems in a Compact Tactical Package," Final Technical Report for U.S. Army Research Laboratory, PSD under contract DAAL01-91-K-0152.

[8] F. Davanloo, C.B. Collins, and F.J. Agee, IEEE Trans. Plasma Sciences, 26, 1463 (1998).

[9] J. P. O'Loughlin and R. P. Copeland, " Conference Record of the 1992 Twentieth Power Modulator Symposium, 1992, pp. 351-354.

[10] W. C. Nunnally, "Photoconductive Pulse Power Switches," Proceedings of the 4th International Pulsed Power Conference, 1983, pp. 620-623.

[11] M. D. Pocha and R. L. Druce, IEEE Trans. Electron Devices, 37, 2486 (1990).

[12] D. L. Borovina, R. K. Krause, F. Davanloo, C. B. Collins, F. J. Agee and L. E. Kingsley, "Switching the Stacked Blumlein Pulsers: Status and Issues," Proceedings of the 10th International Pulsed Power Conference, 1995, pp. 1394-1399.

[13] F. J. Zutavern, G. M. Loubriel, W. D. Helgeson, M. W. O'Malley, R. R. Gallegos, A. G. Baca, T. A. Plut, and H. P. Hjalmarson, "Fiber-optic Control of Current Filaments in High Gain Photoconductive Semiconductor Switches," Conference Record of the 1994 Twenty-First Power Modulator Symposium, 1994, p. 116.

[14] C. B. Collins, F. Davanloo, D. R. Jander, T. J. Lee, H. Park, and J. H.You, J. Appl. Phys. 69, 7862 (1991).

[15] C. B. Collins, F. Davanloo, T. J. Lee, J. H. You, and H. Park, "Amorphic diamond films produced by laser ablation," Mat. Res. Soc. Symp. Proc. 285, 547, 1993.

[16] C. B. Collins, F. Davanloo, T. J. Lee, H. Park, and J. H. You, J. Vac. Sci. & Technol. B11, 1936 (1993).

[17] F. Davanloo, T. J. Lee, D. R. Jander, H. Park, J. H. You, and C. B. Collins, J. Appl. Phys. 71,1446 (1992).

[18] C. B. Collins, F. Davanloo, T. J. Lee, D. R Jander, J. H. You, H. Park, and J. C. Pivin, J. Appl. Phys. 71, 3260 (1992).

[19] C. B. Collins, F. Davanloo, J. H. You, and H. Park, "Nanophase Diamond Films Produced by Laser Deposition," in Laser Applications, Arthur A. Mak, Editor, Proc. SPIE 2097, 129, 1994.

[20] F. Davanloo, T. J. Lee, J. H. You, H. Park, and C. B. Collins, Surf. Coat. Technol. 62, 564 (1993).

[21] F. Davanloo, H. Park and C.B. Collins, J. Mat. Res.11, 2042 (1996).

[22] C. A. Spindt, I. Brodie, L. Humphrey and E. R. Westerberg, J. Appl. Phys. 47, 5248 (1976).

[23] E. A. Koronova and S. A. Sherchenco, Sov. Phys. Semicond. 1, 299 (1967).

[24] N. Konofaos, and C. B. Thomas, J. Appl. Phys., 81, 6238 (1997).

[25] V. S. Veerasamy, G. A. J. Amaratunga, J. S. Park, H. S. MacKenzie and W. I. Milne, IEEE Trans. Electron Devices, 42, 577 (1995).

[26] V. S. Veerasamy, G. A. J. Amaratunga, J. S. Park, W. I. Milne, H. S. MacKenzie and, D. R. McKenzie, Appl. Phys. Lett., 64, 2297 (1994).

[27] L. K. Cheah, X. Shi, E. Liu and J. R. Shi, Appl. Phys. Lett., 73, 2473 (1998).

[28] K. M. Krishna, T. Soga, T. Jimbo and M. Umeno, Carbon 37, 531 (1999).

[29] Mort and K. Okumura, Appl. Phys. Lett., 56, 1898 (1990).

[30] A. Mar, G. M. Loubriel, F. J. Zutavern, M. W. O'Malley, W. D. Helgeson, D. J. Brown, H. P. Hjalmarson, A. G. Baca, R. L. Thornton, and R. D. Donaldson, "Doped Contacts for High-Longevity Optically Activated, High Gain GaAs Photoconductive Semiconductor Switches," Proceedings of the 12th International Pulsed Power Conference, 1999, pp. 303-306.

[31] N. Islam, E. Schamiloglu, C. B. Fleddermann, J. S. H. Schoenberg, and R. P. Joshi, "Improved Hold-Off Characteristics of GaAs Photoconductive Switches Used in High Power Applications", in Proceedings of the 12th International Pulsed Power Conference, 1999, pp. 316-319.